LBL-3107
c.2

EFFECT OF PROCESSING ON MICROSTRUCTURE AND MECHANICAL BEHAVIOR OF MAGNESIUM OXIDE

Truett Belin Sweeting
(M.S. Thesis)

August, 1974

Prepared for the U. S. Atomic Energy Commission
under Contract W-7405-ENG-48

TWO-WEEK LOAN COPY

This is a Library Circulating Copy which may be borrowed for two weeks. For a personal retention copy, call Tech. Info. Division, Ext. 5545

LAWRENCE BERKELEY LABORATORY
UNIVERSITY OF CALIFORNIA
BERKELEY

LBL-3107
c.2

DISCLAIMER

This document was prepared as an account of work sponsored by the United States Government. While this document is believed to contain correct information, neither the United States Government nor any agency thereof, nor the Regents of the University of California, nor any of their employees, makes any warranty, express or implied, or assumes any legal responsibility for the accuracy, completeness, or usefulness of any information, apparatus, product, or process disclosed, or represents that its use would not infringe privately owned rights. Reference herein to any specific commercial product, process, or service by its trade name, trademark, manufacturer, or otherwise, does not necessarily constitute or imply its endorsement, recommendation, or favoring by the United States Government or any agency thereof, or the Regents of the University of California. The views and opinions of authors expressed herein do not necessarily state or reflect those of the United States Government or any agency thereof or the Regents of the University of California.

EFFECT OF PROCESSING ON MICROSTRUCTURE AND MECHANICAL BEHAVIOR OF MAGNESIUM OXIDE

Table of Contents

		Page
I.	INTRODUCTION	1
II.	LITERATURE SURVEY	3
	A. Fabrication of Hot-Pressed MgO	3
	B. Mechanical Behavior	4
III.	EXPERIMENTAL PROCEDURE	10
	A. Characterization of MgO Powders	10
	B. Powder Preparation	16
	C. Specimen Preparation for Mechanical Testing	17
	D. Mechanical Testing	20
IV.	RESULTS AND DISCUSSION	23
	A. Microstructure Development	23
	(1) Effect of Powder Preparation on Microstructure	23
	(2) Characterization of Test Specimens	27
	B. Mechanical Behavior	39
V.	SUMMARY AND CONCLUSIONS	51
ACKNOWLEDGMENTS		53
REFERENCES		54

EFFECT OF PROCESSING ON MICROSTRUCTURE AND MECHANICAL BEHAVIOR OF MAGNESIUM OXIDE

Truett Belin Sweeting

Inorganic Materials Research Division, Lawrence Berkeley Laboratory
and Department of Materials Science and Engineering,
College of Engineering; University of California,
Berkeley, California 94720

ABSTRACT

Specimens of polycrystalline MgO were fabricated from two different MgO powders by hot pressing in graphite and alumina dies, followed by annealing in air, vacuum, or within the graphite die in vacuum. The two powders were prepared by dispersing in isopropanol, drying, and milling in a rubber-lined mill with alumina balls. The relatively high cation content, particularly Ca and Si, in Type II MgO was the most significant difference in the two powders as it led to the formation of a small amount of liquid phase along the grain boundaries during the annealing step at 1550°C.

Impurities introduced and modified throughout the entire processing procedure of powder preparation, pressing in a graphite die, and annealing in different ambient atmospheres resulted in microstructures with varying grain size and grain boundary structure in the specimens produced from Type I MgO. The formation of a liquid phase in the Type II MgO specimens tended to eliminate the effect of these processing variables but led to the development of grain sizes two or three times larger in size.

Correlations of the microstructures of the specimens were made with their mechanical behavior in compression at a constant strain rate at 1200°C. The Type I specimens had considerably higher yield and maximum

stresses than the Type II. Also, the specimens annealed in air had the largest strain at failure, and the ones annealed in the graphite die had the smallest; this behavior was attributed to a more perfect grain boundary for the former. The Type II specimens failed at considerably lower stresses and failures with little differences in value with different annealing atmospheres which was attributed to the presence of the brittle phase along the grain boundaries.

I. INTRODUCTION

In recent years, there has been considerable interest in design of ceramics for applications in severe environments. The ability of ceramics to maintain loads at high temperatures and to resist oxidizing atmospheres has made them desirable over metals in such situations. However, the inherent brittleness of many ceramics has made designing with them a very difficult task and thus has limited their applications. A degree of ductility, which is favorable for design applications, has been observed in many single crystal ceramic materials; however, the inability of most polycrystalline ceramics to satisfy the criteria proposed by Von Mises, that five independent slip systems be operative for general deformation to occur, has limited their ductility. Cubic ionic polycrystalline materials, such as MgO, have been found to satisfy this criteria at high temperatures, and therefore have been the subject of considerable investigation.

In the study of the mechanical properties of a polycrystalline material, it is essential to understand the functional role of microstructural features, because these are the critical parameters which determine the material's behavior. In addition to single crystal investigations, considerable work has been done in this laboratory on polycrystalline MgO. These studies focused on interpreting stress-strain curves in terms of such features as pore size, amount and distribution, grain size and shape, and amount of second phase. However, little work has been done on studying and controlling the effects of processing on these microstructural features. Also, the results of the reported studies have pointed out the need for a further investigation into the nature of

the grain boundary and its effect on mechanical behavior. Therefore, it is the objective of this study to investigate the role of processing conditions on development of microstructure, and to determine the relation between such microstructural features and mechanical behavior with particular emphasis placed on the significance of the nature of the grain boundary.

II. LITERATURE SURVEY

A. Fabrication of Hot-Pressed MgO

The fabrication of dense, fine grained MgO has been accomplished by hot pressing, and there have been several investigators who have studied various hot-pressing techniques to produce such specimens. Murray, Livey, and Williams[1] described the principles of hot pressing and presented data on a number of ceramic materials. Vasilos and Spriggs[2] hot pressed MgO over a range of temperatures and pressures in both graphite and alumina dies, and concluded from determined diffusion coefficients and activation energies that beyond the initial stages densification was a diffusion-controlled process. Spriggs et al.[3] investigated the hot pressing of several oxides in alumina dies and produced nearly theoretically dense MgO at 1120°C and 13,000 psi. The preparation and hot pressing of high purity MgO has been described by Leipold and Nielson.[4] They obtained theoretically dense specimens at 800°C and 10,000 psi; in addition, these specimens showed rapid grain growth and no reheat porosity on subsequent heating in air.

LiF additions to MgO have been used to produce optically transparent specimens. Rice[5] developed a technique which has been modified by others[6,7] to produce such samples in a two-step process of vacuum hot pressing followed by annealing in air. The mechanisms of densification in this process have been described by Hart, Atkin and Pask.[8]

The influence of water vapor on the hot pressing of MgO was studied by Shelly and Nicholson.[9] It was found to aid in the initial stage of densification by a fluidized bed effect which caused rearrangement; the overall effect, however, was to inhibit densification due to back

pressure exerted by the water vapor entrapped in pores. Leipold and Kapadia[10] studied the effect of the anions, S^{2-}, CL^{-}, F^{-} and OH^{-}, on the hot pressing of MgO and found that they all retarded densification, with the effect decreasing in the order listed. It was shown that this effect was due to gas pressures developed within the compact and die cavity by demonstrating that the vapor pressure of the species and its solubility in the MgO lattice determined the magnitude of the retardation effect. Rice[11] studied the effect of gaseous impurities on the hot pressing and behavior of MgO, CaO, and Al_2O_3. Using infra-red and mass spectroscopy, hydroxide and carbonate impurities were shown to exist in MgO hot pressed with and without LiF which persisted on reheating in air up to temperatures near 1100°C; bloating and clouding were also found to occur in these specimens, which was attributed to pressure building up from the entrapped gases. Similar observations were reported by Nielson and Leipold,[12] and Day and Stokes.[13] Impurity distributions in hot-pressed MgO has been studied by Leipold,[14] and the impurities Al, Si and Ca were found to segregate at grain boundaries even when present in amounts as low as 30 ppm.

B. Mechanical Behavior

Investigations of the mechanical behavior of single crystal MgO have been the basis for polycrystalline studies through development of the theories for dislocation movement. Early work on single crystals was focused on determining room temperature mechanical properties. The first studies[15,16] demonstrated that ductility was possible in ionic solids in NaCl-type structures. Other room temperature studies investigated the effect of heat treatment and impurities on strength,[17] nucleation of

cracks in tension,[18] bending,[19-21] and compression,[22] importance of surface condition[23-25] and the effects of fresh and grown-in dislocations on yield stress and crack nucleation.[26,27]

May and Kronberg[28] extended single crystal studies to elevated temperatures by studying the temperature dependence of yield stress in bending to 1000°C. Results were discussed in terms of dislocation interactions with impurities. Hulse and Pask[29] continued single crystal studies at high temperature by deforming crystals with a <100> loading axis in compression at a constant loading rate from -196°C to 1200°C. The bulk yield stress decreased exponentially with temperature to 900°C and then remained essentially constant to 1200°C. Deformation occurred on (110) planes, and slip on one set of planes had difficulty in passing through slip bands on the conjugate set of planes. Later, Hulse et al.[30] performed a similar study on crystals oriented with <110> and <111> loading axis. Reasonable agreement was found with expected results from analysis of the critical resolved shear stress arising on the slip systems. <100> and <110> loading axis produces resolved shear stresses on four of the six (110) slip systems; however, the stress for the <100> axis is one-half the applied stress, whereas for the <110> axis the resolved shear stress is one-fourth of the applied stress. Results showed the yield stress for the (110) axis to be about twice that obtained by Hulse and Pask[29] for <100>, in good agreement with the analysis.

The <111> loading axis does not produce a shear stress on the (110) slip systems, and etching revealed slip to occur on (100) <110> systems. As expected, the yield stress was much higher for this axis due to the stronger electrostatic repulsions for dislocation movement on the (100)

planes. Copley and Pask[31] extended this work by compression testing to 1600°C. Day and Stokes[32,33] tested single crystal MgO in tension with a <100> and <110> loading axis in the range 1000°C-2000°C, and found behavior to be determined by the number of slip systems operating in a given volume, which was shown to be dependent on temperature and strain rate.

Miles et al.[34] studied the flow stress and pinning stress of single crystal MgO in bending, over a range of temperatures. It was found that the mechanism controlling behavior at high temperatures was a combination of continual pinning caused by deformation, and thermally activated unpinning. The effect of iron impurity and its oxidation state on the compressive yield stress of MgO single crystals over a range of temperature has been investigated by Moon and Pratt.[35] A recent work by Srinivas and Stoebe[36] emphasized the importance of impurity and heat treatment on the behavior of MgO single crystals, and investigated yielding and work hardening as a function of temperature for crystals of varying impurity. Results were explained in terms of dislocation interactions with impurities.

Bicrystals have also been used to study the deformation of MgO. Their primary uses have been to study dislocation interactions with grain boundaries[27,37,38] and also to study grain boundary sliding.[39-42]

Studies of the behavior of polycrystalline MgO have been concerned primarily with establishing relationships between microstructural features and mechanical properties. Stokes and Li[27] studied the behavior of polycrystalline MgO in tension at room temperature and found the number of mobile dislocation sources to be critical in controlling

strength. Specimens prepared free of such sources were nearly twice as strong as specimens containing mobile dislocations. Vasilos et al.[43] found the strength of MgO tested in bending to decrease with grain size, with the effect diminishing as temperature increased. From etch pit studies it was concluded that a dislocation mechanism was operating at elevated temperatures. Day and Stokes[44] produced samples with grain boundaries free of porosity and impurities by recrystallization of MgO single crystals. These samples, and ones prepared by hot pressing, were tested in tension up to 2200°C. Deformation in both types of samples was controlled by dislocation glide and climb; however, the brittle-ductile transition temperature of 2200°C for the hot-pressed specimens was 500° higher than that for the recrystallized material. Grain boundary sliding and grain boundary migration phenomena were noted.

Five different types of polycrystalline MgO were studied in compression to 1400°C by Copley and Pask.[6] The behavior of each type was explained in terms of its microstructure, and it was concluded that ductility could be achieved in compression when slip could be initiated homogeneously, resistance to dislocation movement was low, and grain boundaries were strong enough to resist separation. Further work by Langdon and Pask[45] showed that pore size and distribution, and impurity concentration at the grain boundaries were critical factors in determining the behavior of polycrystalline MgO. Plasticity below 1200°C was attributed to strong grain boundaries which allowed build-up of sufficient stress concentrations to nucleate slip on the (100) system, thereby providing the necessary five independent systems required for general deformation.

Evans and Davidge[46] studied the strength and fracture of polycrystalline MgO in bending at room temperature, and showed that the surface condition determined the strength and fracture mode. Samples tested in the as-machined condition failed by extension of pre-existing flaws, whereas in chemically polished specimens failure was initiated by plastic flow. This work was extended to high temperatures by Evans et al.[47] Fracture mode at any given temperature was observed to be controlled by grain size, surface finish, quantity and size of pores, and quantity and distribution of the impurity.

The results of Snowden and Pask[48] emphasized the importance of the grain boundary structure in the mechanical behavior of MgO. Specimens fabricated by different procedures, yet having similar microstructures with the exception of grain boundary porosity and purity, behaved quite differently in compression at 1200°C. Behavior was interpreted in the manner of Langdon and Pask[45] in that specimens free of boundary porosity and impurities thereby possessing strong grain boundaries, yielded at lower stresses and exhibited higher strain at fracture based on the proposed mechanism of initiation of slip on (001) $\langle 1\bar{1}0 \rangle$ system by stress concentrations. Snowden[49] also studied the effect of a calcium-magnesium-silicate (CMS) second phase on the stress-strain behavior in compression of MgO. For a given temperature, the amount and distribution of the second phase was shown to be critical. A review of the high temperature behavior of ceramics has been presented by Radford and Terwilliger.[50,51]

Microstructural inhomogenities are important in the mechanical testing of materials since such defects as local collected porosity can act as stress raisers leading to initiation or propagation of flaws, thus

producing premature failure. There is little discussion of this in the literature; Bennett and Niesz,[52] however, did report an increase in bend strength of 13% in sintered alumina upon removal of such non-uniformities.

III. EXPERIMENTAL PROCEDURE

A. Characterization of MgO Powders

Two magnesia powders were used in this study, and will hereafter be referred to as Type I and Type II. Both powders were characterized to exemplify differences between them.

The powders were analyzed for both the cation and anion impurities, and these results are shown in Table I. The cations except for Si were determined spectrographically* and the Si and anion content were determined by wet chemical means.** As indicated, the major difference in cations was the high Si and Ca content of Type II. The anion analysis showed both powders to contain a substantial amount of carbonate and hydroxide; in addition, Type II contained a much higher amount of sulfate. On the basis of the anion percentages obtained, and assuming the carbonate and hydroxide to exist as $MgCO_3$ and $Mg(OH)_2$, the actual percentages of these compounds were calculated, and are shown in Table I.

After ignition, the powders were 99.7% and 99.2% MgO respectively. Differential thermal analysis (DTA), and thermogravimetric analysis (TGA) were performed on both powders, and the results for Type I and Type II are shown in Figs. 1 and 2 respectively. The DTA was obtained in air at a heating rate of 10°C/min up to 1000°C; it showed endotherms beginning about 265°C and peaking at 360°C for both types of MgO which is in good agreement with the results of Chown and Deacon[53] for hydrated magnesia. The TGA was also run in air at 10°C/min up to 1000°C and showed weight

---

* Lawrence Berkeley Laboratory, Univ. of Calif., Berkeley, Calif.
**Merck and Co., South San Francisco, Calif.

Table I. Chemical analysis of MgO powders*

Constituent	Type I	Type II
Al	.07	.02
Ca	.05	.30
Fe	.07	.05
Na	.01	.005
Si	.045	.18
Cl^-	.005	.021
$SO_4^=$	.01	.22
$CO_3^=$	.71	.82
OH	2.64	2.48
Loss on ignition	3.74	3.82
% as $MgCO_3$	1.35	1.57
% as $Mg(OH)_2$	8.6	8.8

*Cation and anion results are in percent of the element or radical.

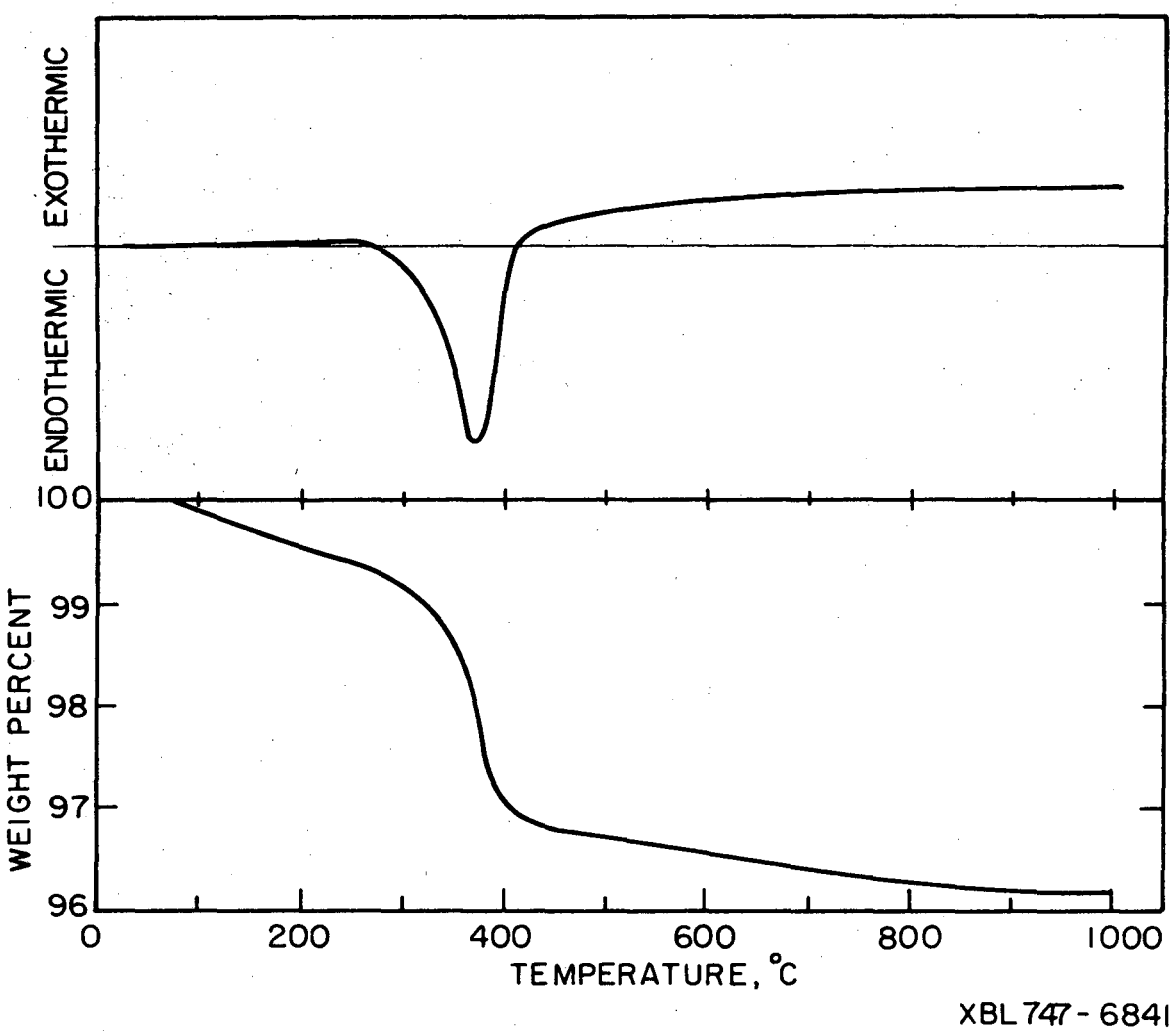

Fig. 1. DTA (top) and TGA results for Type I MgO powder.

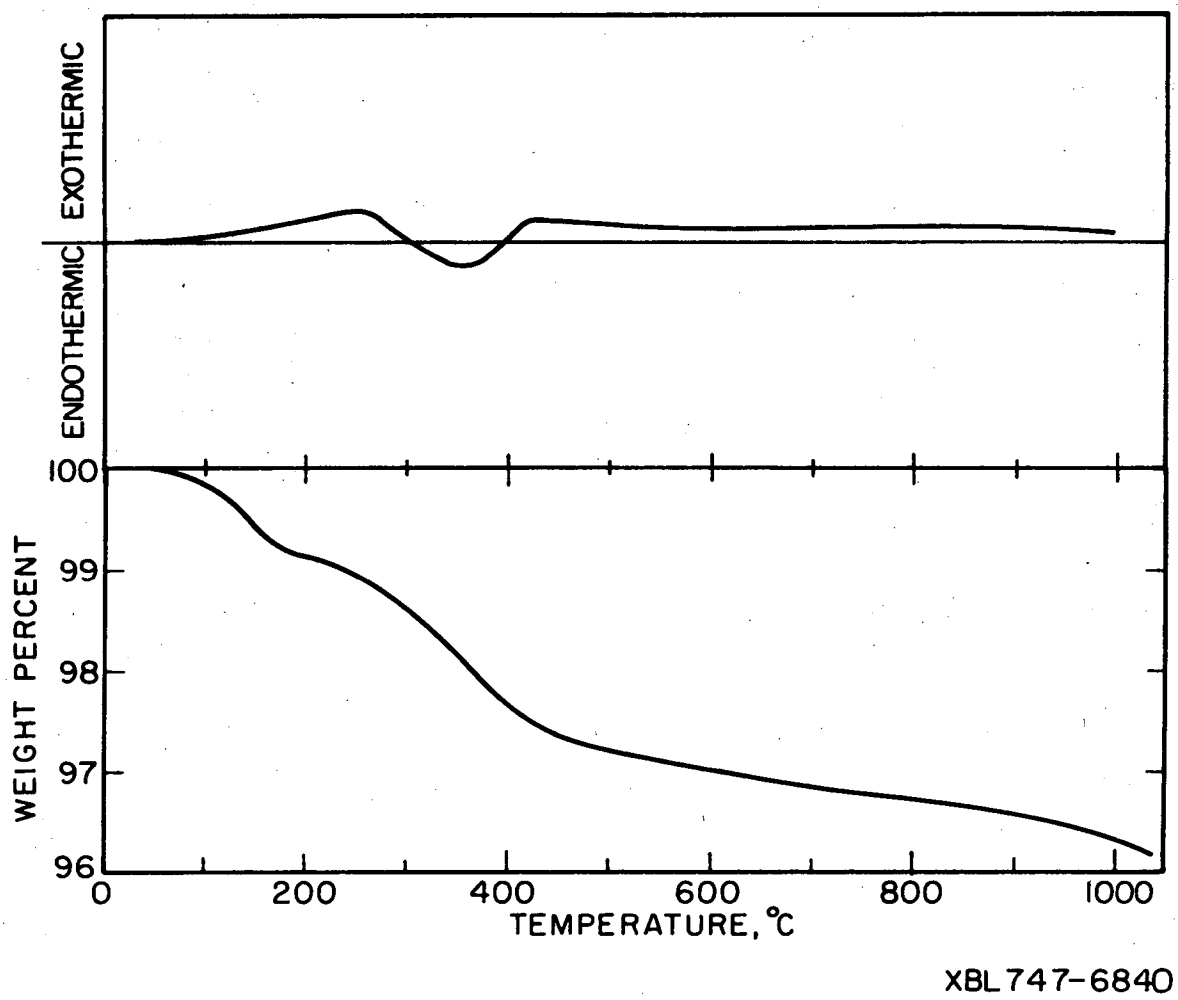

Fig. 2. DTA (top) and TGA results for Type II MgO powder.

losses at temperatures which corresponded well with the observed DTA peaks. These results indicated that the Type II powder does not lose its combined hydroxide as readily as Type I as indicated by the slope of its TGA curve and the broadness of its DTA peak. Type II was still losing weight at 1000°C whereas Type I had nearly stabilized. This high temperature weight loss could also be due to the higher sulfate content which decomposes near 1100°C.

Table II contains physical data obtained on the MgO powders. The surface area was measured by adsorption from an iodine solution.* The amount of iodine adsorbed by the powder was determined by titration, and this was related through a standard curve to an equivalent B.E.T. surface area. The reactivity was measured* by mixing two grams of powder with citric acid and noting the time to endpoint using phenolphthalien as an indicator, a shorter time being indicative of greater reactivity. These tests pointed out a major difference in the physical characteristics of the powders; Type II was twice as reactive and had five times the surface area of Type I.

X-ray diffraction patterns of both powders did not indicate the presence of any second phase, including $MgCO_3$ and $Mg(OH)_2$. The crystallite size shown in Table II was determined by a method outlined by Rau[54] using the Scherrer equation, and the results showed Type I to have a higher degree of crystallinity.

---

*Performed by Merck and Co., South San Francisco, Calif.

Table II. Physical characteristics of MgO powders

	Type I	Type II
Surface area M^2/g	11.5	56.5
Reactivity (sec)	87	44
X-ray crystallite Size (Å)	360	120

Table III. Green and hot-pressed densities; grain size and density after annealing for Type I MgO specimens produced by different processing techniques

Procedure	Green Density	Hot Pressed Density	Annealed Density	Grain Size
Unmilled	34	98.0	97.8	32
(1) Dry milled - alumina balls	39	98.0	97.8	30
(2) Dispersed, dry milled - alumina balls	46	98.5	98.2	28
(3) Dry milled - teflon balls	39	96.5	96.2	21
(4) Wet milled, dry milled - Teflon balls	41	95.5	95.1	19

B. Powder Preparation

Preliminary specimens prepared from an unmilled powder were found to contain undesirable microstructural inhomogenities which were attributed to agglomeration in the starting powder. This led to an investigation into the following powder processing procedures, using Type I powder to evaluate their effectiveness in reducing such defects.

(1) Dry milled 2 hours--alumina balls.

(2) Dispersion in isopropanol, dried, dry milled 2 hours--alumina balls.

(3) Dry milled 2 hours--teflon balls.

(4) Wet milled 1 hour, dried, dry milled 2 hours--teflon balls.

In each case the starting powder was first screened to remove the coarsest aggregates.

The ball milling was done in a 2-liter, rubber lined mill, using 55 grams of powder in each case. The dispersion step in (2) consisted of gradual addition of the 55 grams of unmilled powder to 275 ml of isopropanol, while stirring magnetically. The resulting mixture was placed in an ultrasonic cleaner for two minutes to aid dispersion. The suspension was then dried 24 hours at 90°C. The result was a "cakelike" structure which was broken up manually before ball milling. In (4) the powder was dispersed as in (2), but an additional 250 ml of isopropanol was added during dispersion; this mixture was wet milled one hour before drying within the mill for 24 hours at 90°C. This treatment was followed by the dry milling step.

The powders were then hot pressed in graphite dies and annealed in air as described in IIIC; the resulting microstructures were analyzed

to determine the ability of the various procedures to reduce inhomogenities. Procedure (2) was selected as the best method of preparation. A complete discussion of the microstructures appears later.

C. Specimen Preparation for Mechanical Testing

Types I and II MgO powders were prepared for hot pressing according to processing technique (2) of dispersion and dry milling as outlined above. Both powders were hot pressed in graphite and alumina dies.

With the graphite die, a thin (.005") graphite paper sleeve was used along the die cavity wall to reduce friction and wear on the die and plungers. Graphite paper spacers were also used between the powder and the plunger faces. The powder was placed in the die and cold pressed at 2000 psi outside of the furnace, so that measurements could be taken to determine green density. The die was placed in the hot press, and evacuated to 10^{-4} Torr before heating. The heating cycle consisted of heating at 8°C/min to 500°C and holding 15 minutes to allow gas from decompositions to escape. The heating was then continued to 1000°C and held for one hour, also to allow sufficient time for the removal of gases from the system. This was followed by heating to 1250°C and holding for 30 minutes. A pressure of 3000 psi was applied at 1200°C and maintained constant through the hold at 1250°C. Pressure was then released and the specimen was furnace cooled. A similar procedure was followed for the alumina die; however, the heating rate was reduced to minimize thermal gradients across the die wall. Also, molybdenum spacers were used to separate the powder from the plunger faces to prevent sticking and reaction. Because of the low density of the Type I MgO specimen produced by this procedure, a second run was made applying pressure at 1100°C, and

gradually increasing it to a maximum of 6500 psi at 1200°C. The pressure was then held constant to 1250°C and held 20 minutes. The resulting disks were cut into specimens approximately .6 in. x .25 in. x .25 in., using a diamond blade.

The Type II powder showed different hot pressing characteristics than Type I. A plot of density versus temperature obtained from the measurements of ram travel, for both powders hot pressed in the graphite die is shown in Fig. 3. Densification began for both powders near 800°C, with Type II showing a much more pronounced effect. From the hold at 1000°C to application of pressure at 1200°C, little densification occurred for Type I; Type II, however, showed a very rapid increase in density. Upon application of pressure, Type II reached its final density after only a few minutes, and before the final hold temperature of 1250°C was reached. Type I was still densifying at 1250°C, and continued until near the end of the 30 minute hold period. The higher surface area and greater reactivity of the Type II powder is a possible explanation for this behavior since these factors lead to shorter diffusion distances and increased particle-particle contact, thereby resulting in greater densification rates. Another possible explanation is the formation of a liquid phase. Rice[5] has suggested the possibility that Ca impurities in MgO could form $Ca(OH)_2$ and $CaCO_3$ as non-decomposing liquids which form eutectics with CaO in the 500-700°C range. He pointed out that this liquid could aid densification since MgO has been shown to have limited solubility in these liquids.

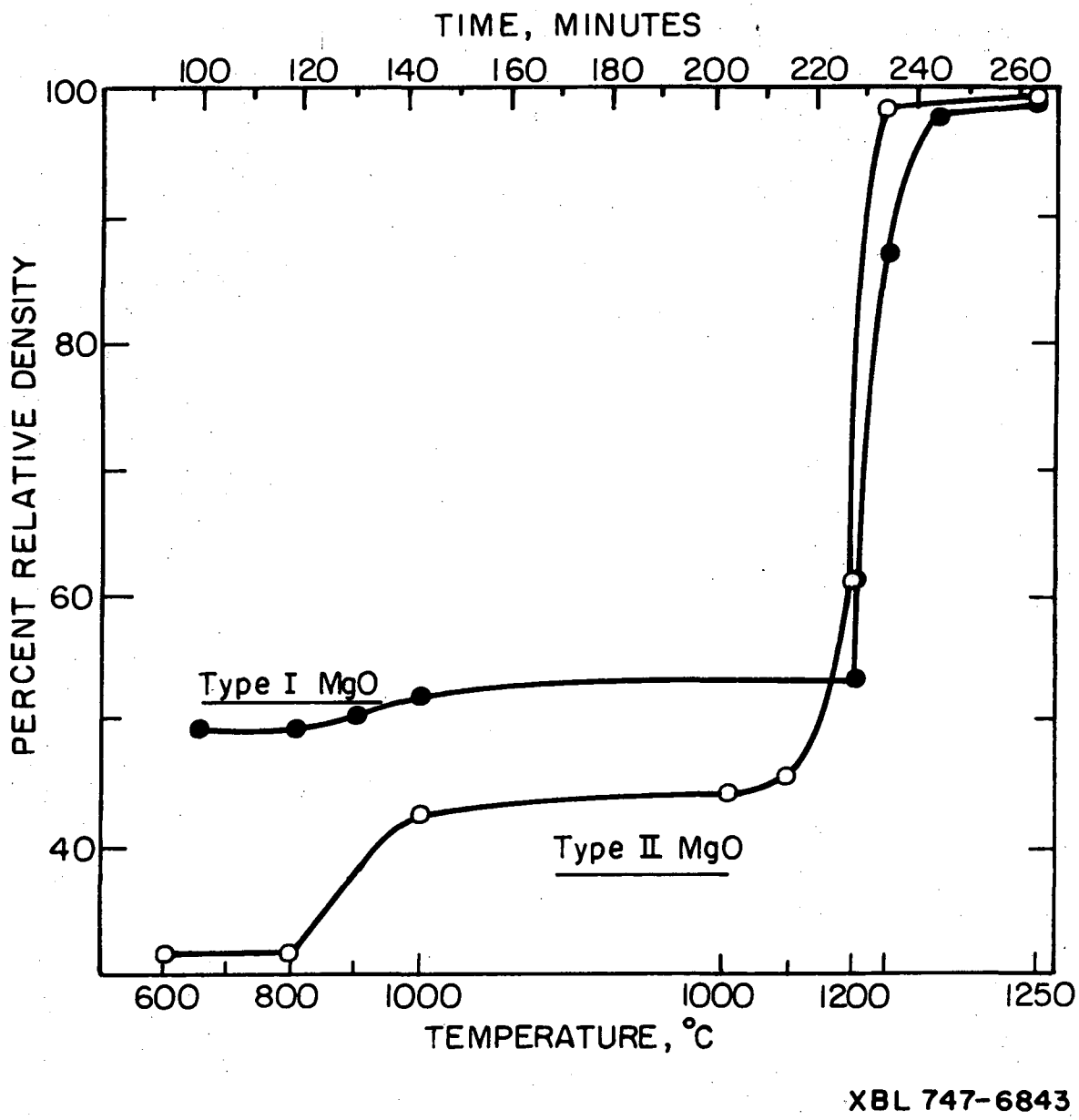

XBL 747-6843

Fig. 3. Density versus temperature and time for Types I and II MgO specimens during hot pressing in graphite die.

Type I and Type II samples from the graphite die were annealed at 1550°C for two hours in air, vacuum, and vacuum within the graphite die. The annealing in air was done in a platinum crucible in a quench furnace with $MoSi_2$ elements. The vacuum anneal was also done in a platinum crucible using a Brew furnace with tantalum heating elements. The annealing in the graphite die was done in vacuum in the hot press, which had molybdenum heating elements. Samples from the alumina die received identical heat treatments, but were not annealed in the graphite die. All samples were furnace cooled.

Approximately .15 in. was cut from the end of each sample and the internal surface of the end piece was used for microscopic examination. Rough polishing was done using a series of emery papers through grade 4/0. This was followed by polishing on a nylon cloth with 6 μm diamond paste using kerosene as a lubricant. Fine polishing was done on a Syntron vibrator with 1 μm diamonds. All samples were etched using .5 M $AlCl_3$ at 50°C for about one minute. Grain size determinations were made by counting the number of grains in a known area, converting to equivalent spherical diameter, and multiplying by a factor of 1.28. Over 500 grains were counted in each case. Density measurements were made using a displacement technique in mercury; a value of 3.58 was taken as theoretical density of MgO to compute relative densities.

D. Mechanical Testing

Specimens for the mechanical testing had a length to width ratio of 2:1 and were approximately .18 in. x .18 in. x .36 in. The specimens were polished to these dimensions on a series of emery papers using a jig designed to keep faces parallel. Special care was taken on the ends

to make sure they were flat, parallel, and perpendicular to the loading axis. Following this polishing, the specimens were chemically polished in 85% orthophosphoric acid at 110°C for two minutes.

All stress-strain data was obtained in compression at 1200°C at a constant strain rate of .025/min based on original sample height using an Instron testing machine. The specimen was heated electrically with $MoSi_2$ elements at about 10°C/min, with a stabilization period of approximately 20 minutes at 1200°C. A schematic diagram of the specimen arrangement in the furnace is shown in Fig. 4. The platinum foil prevented reaction between the specimen and the Lucalox Al_2O_3 buttons. The collar was used to maintain alignment and to prevent sideways motion of the Al_2O_3 buttons during testing. The specimen temperature was taken from the thermocouple touching the alumina button. All stresses reported are based on original cross-sectional area, and all strains are true strains calculated from the recorded engineering strain. The amount of plastic strain was taken from the .2% offset yield stress to the maximum stress recorded. The tests were run until the load started decreasing at an accelerating rate.

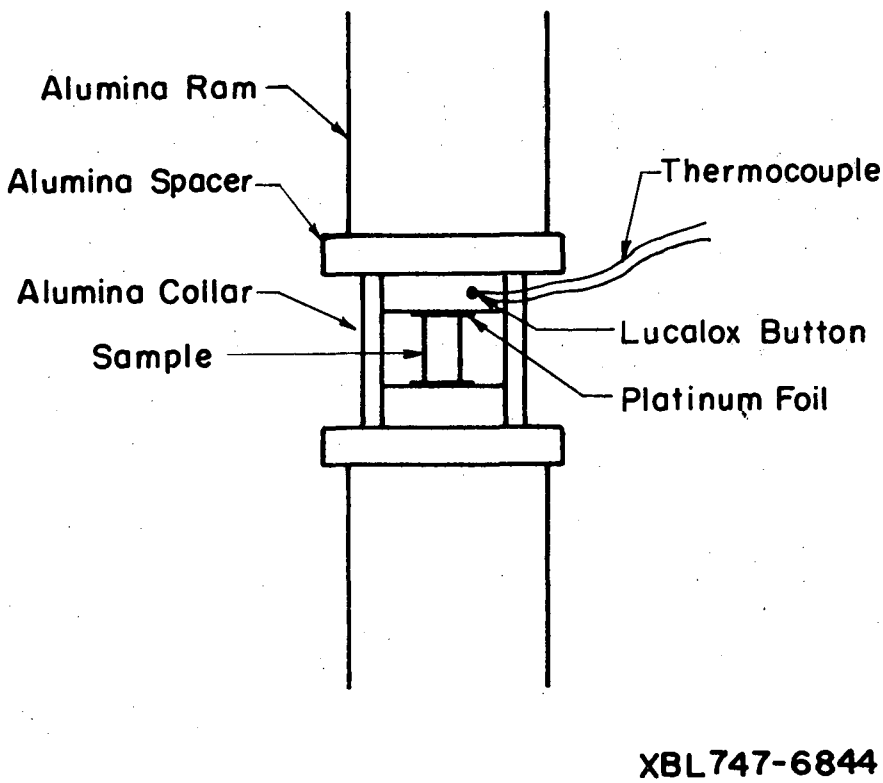

Fig. 4. Specimen arrangement in furnace for stress-strain testing.

IV. RESULTS AND DISCUSSION

A. Microstructure Development

(1) Effect of Powder Preparation on Microstructure

The green density, as hot-pressed density, and the density and grain size of Type I MgO specimens after annealing in air fabricated by the powder preparations investigated are summarized in Table III. Shown in Fig. 5 is a micrograph of a specimen prepared from the unmilled powder illustrating the presence of regions of higher porosity and smaller grain size that warranted the use of a milling procedure to aid homogeneity. Figures 6-9 show micrographs corresponding to the four processing procedures investigated.

Specimens from procedure (1) and (2) were similar in appearance after hot pressing and had light gray (somewhat lighter in (1)) slightly translucent cores covering approximately four-fifths of the cross sectional area; the remaining areas adjacent to the surfaces were white. In contrast, specimens made from the unmilled powder and procedure (3) produced uniform white cross sections whereas (4) yielded a disk which was very dark gray throughout the entire piece. All specimens were white after annealing in air.

The cores developed in (1) and (2) were attributed to the picking up of organics from the abrasion of the rubber-lined mill by the Al_2O_3 balls; it is interesting to note, however, that this apparently did not interfere significantly with the densification process since after annealing in air, both (1) and (2) had essentially the same density as the specimen prepared from the unmilled powder. In (3), since MgO is harder than teflon, it is expected that the powder would be picking up teflon on

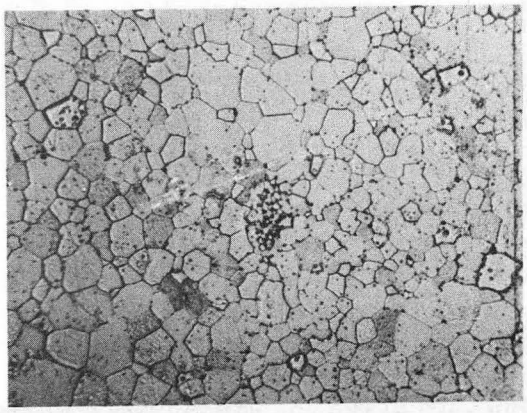

Fig. 5. Micrograph of specimen prepared from unmilled Type I MgO.

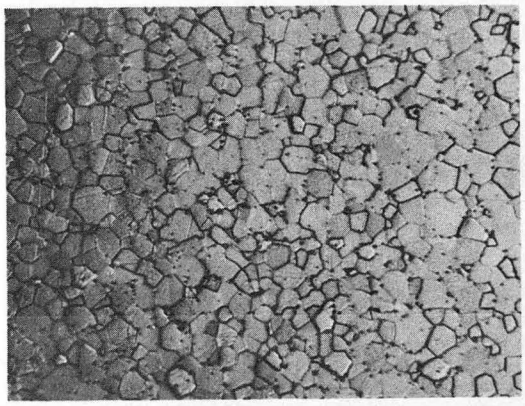

Fig. 6. Micrograph of specimen prepared from Type I MgO by procedure (1).

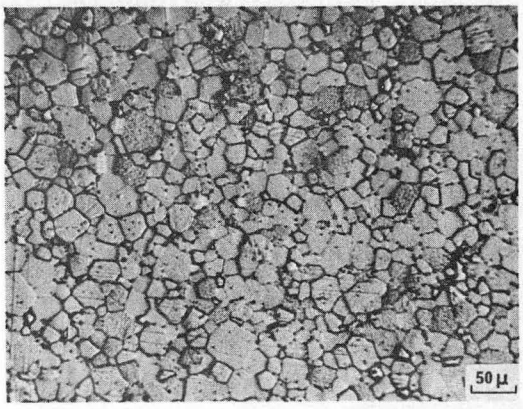

XBB 748-5185

Fig. 7. Micrograph of specimen prepared from Type I MgO by procedure (2).

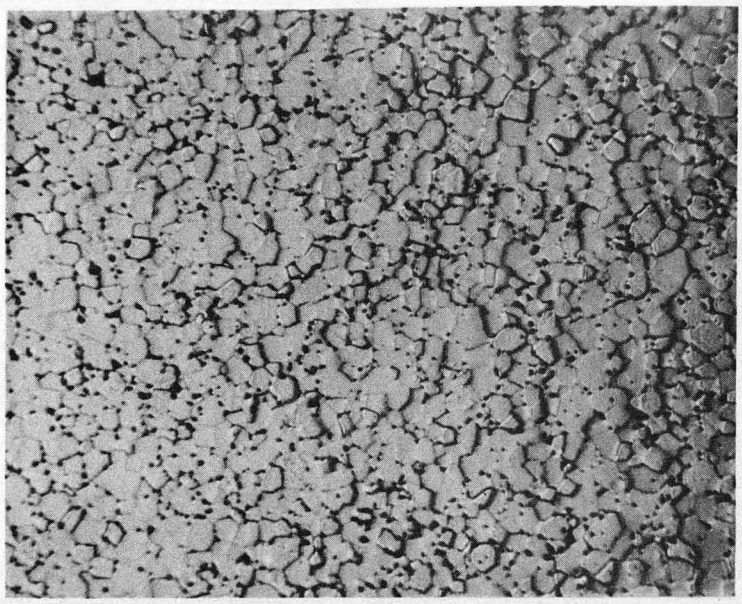

Fig. 8. Micrograph of specimen prepared from Type I MgO by procedure (3).

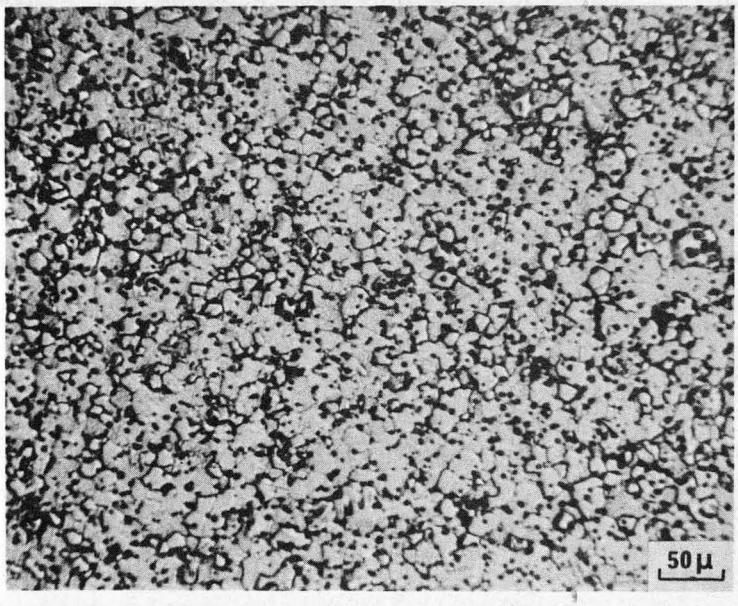

XBB 748-5193

Fig. 9. Micrograph of specimen prepared from Type I MgO by procedure (4).

its surfaces. The data indicate that the presence of teflon significantly reduced density and grain size, but no color change was observed. The darkness of the sample prepared by (4) was again attributed to the picking up of organics from the rubber. In this procedure, the isopropanol was thought to aid the solution of rubber into the mixture during wet milling, possibly by removing plasticizers from the rubber making it brittle and subject to abrasion.

Since (1) and (2) showed a grayish core, but essentially no difference in hot-pressed density from the unmilled specimen, it is expected that during hot pressing the organics decomposed producing a gas which escaped from the system and a residue which produced the gray core. Since the hot pressing was done in vacuum with graphite dies, the residue products of such a reaction were not oxidized. Also, since the gas left the system and was not entrapped, it did not interfere with densification during hot pressing by building up an internal back-pressure, resulting in a relatively high hot-pressed density.

The presence of teflon, procedures (3) and (4), decreases the hot-pressed density significantly, as seen in Table III. The lack of a gray core in (3) indicates a different type of reaction involving only teflon; the dark gray core in (4) was due to rubber pickup as in (1) and (2). The Merck Index[55] reports that teflon reverts to the gaseous monomer at 400°C. It appears that some of the volatilized teflon must have adsorbed on the surfaces of the particles and must have affected the γ_{ss} (grain boundary energy) and γ_{sv} (surface energy) so that densification is retarded in hot pressing.

The annealed density for all specimens was slightly less than their corresponding hot-pressed densities suggesting little variation in build-up of back pressure due to oxidation of the dark gray residue or any adsorbed species. Grain growth, however, was significant in that the grain size for all of the hot-pressed specimens was about 3 μm. Also, of significance is the fact that the retardation of grain growth for the specimens made from powders exposed to teflon ((3) and (4)) was greater than for those specimens exposed to rubber and alcohol, relative to the unmilled powder specimen.

After analysis of the microstructures on the basis of uniformity, density, and grain size, procedure (2), dispersion in isopropanol followed by dry milling with alumina balls was chosen as the best procedure for preparation of specimens for mechanical testing. A discussion of the microstructures prepared for mechanical testing follows.

(2) Characterization of Test Specimens

(a) Type I MgO

Table IV summarizes data on weight loss, density and grain size obtained on Type I MgO specimens fabricated in graphite and alumina dies and annealed in air, vacuum, and in vacuum in the graphite die using procedure (2). Fracture surfaces of the as-hot-pressed specimens are shown in Fig. 10. Optical micrographs of the specimens annealed in different ambient atmospheres are shown in Figs. 11 and 12.

The specimen formed in the graphite die had a grayish core as described previously, whereas both specimens formed in the alumina die were white. This indicated that the nature of the atmosphere during the hot pressing was critical in determining the nature of the adsorbed

Table IV. Grain size density and weight loss data for Type I MgO

Die Used	Treatment	Weight loss %	Density %	Grain size µm
Type I				
Graphite	As hot pressed		98.5	<3
	Air anneal	0.07	98.3	28
	Vacuum anneal	0.27	98.1	28
	Die anneal	2.87	98.3	30
Alumina	As hot pressed (1)		93.0	<3
	Air anneal	0.336	96.0	41
	Vacuum anneal	0.527	96.2	38
	As hot pressed (2)		99.0	<5
	Air anneal		98.6	44
Type II				
Graphite	As hot pressed		99.1	<3
	Air anneal	0.09	98.0	84
	Vacuum anneal	0.45	98.0	90
	Die anneal	2.60	98.5	101
Alumina	As hot pressed		99.0	<5
	Air anneal	0.072	98.0	87
	Vacuum anneal	0.399	98.3	80

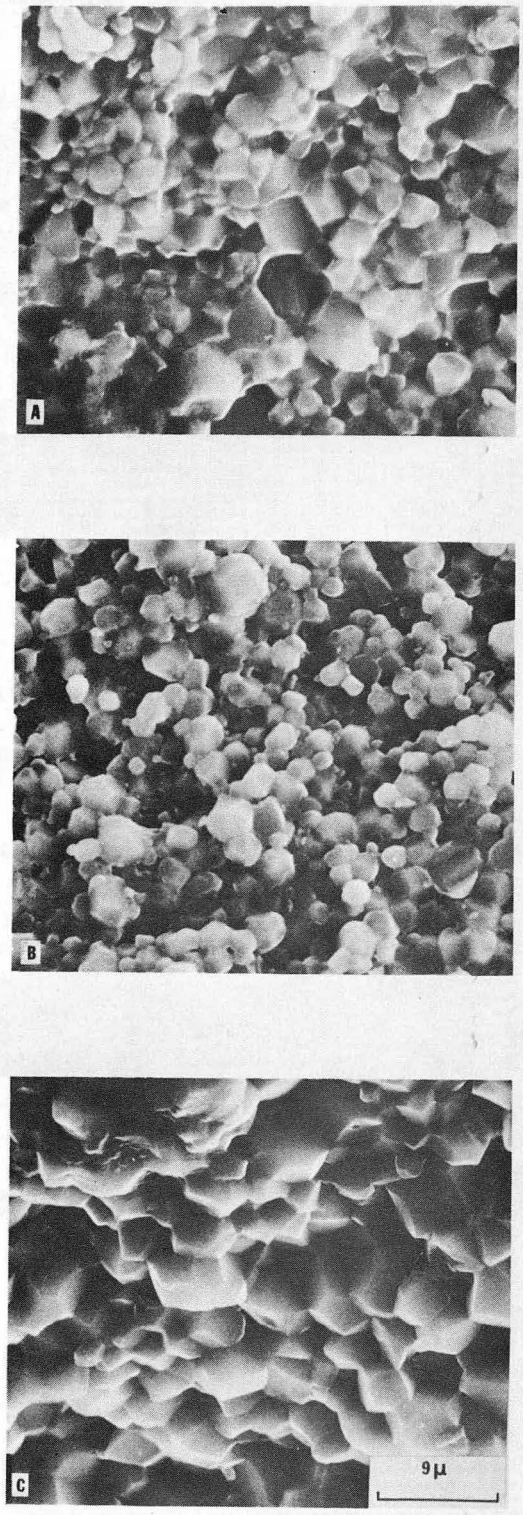

XBB 748-5186

Fig. 10. As-hot-pressed fracture surfaces of Type I MgO specimens: (a) graphite die, (b) low density sample from alumina die, (c) high density sample from alumina die.

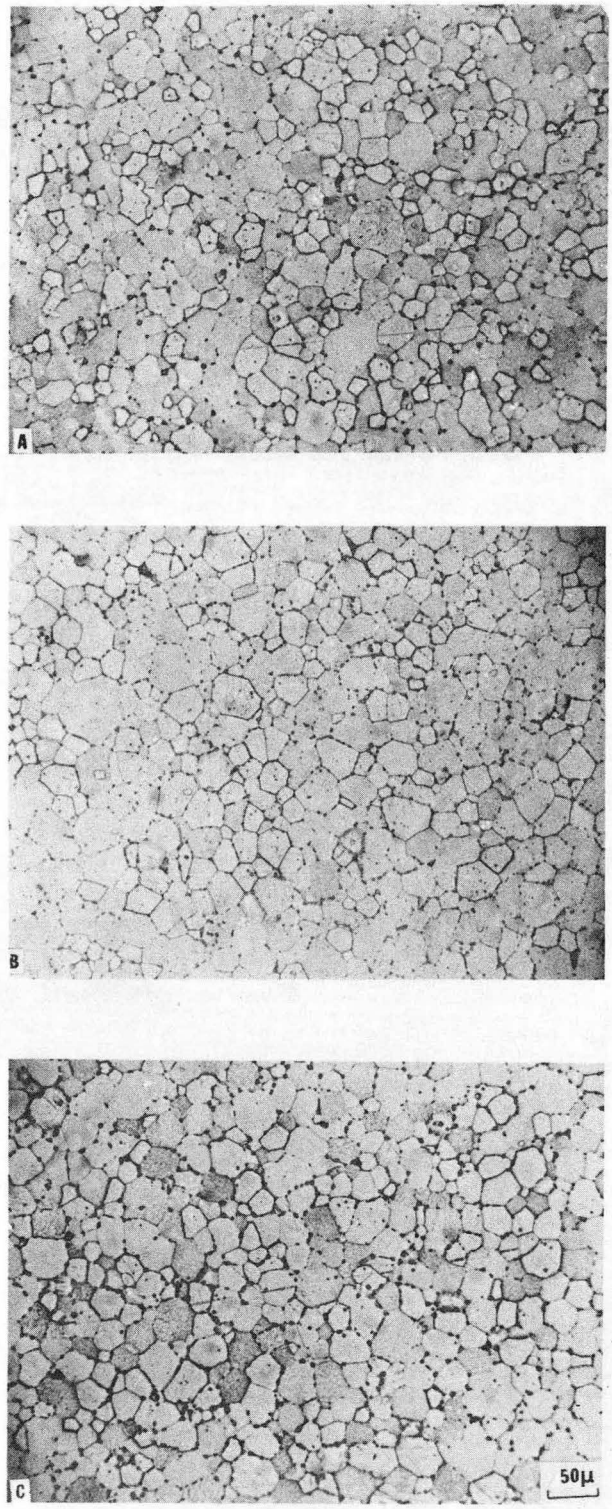

XBB 748-5188

Fig. 11. Micrographs of annealed Type I specimens from graphite die: (a) air anneal, (b) vacuum anneal, (c) vacuum within graphite die.

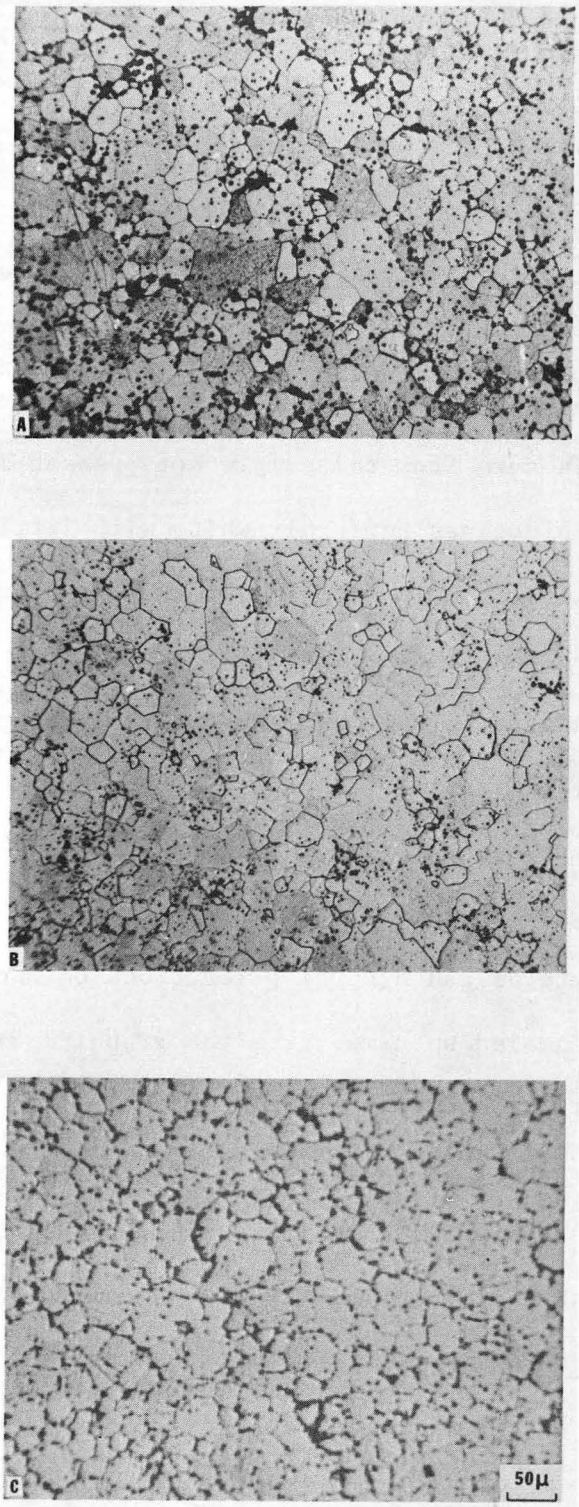

XBB 748-5184

Fig. 12. Micrographs of annealed Type I specimens from alumina die: (a) low density specimen, air anneal, (b) low density specimen, vacuum anneal, (c) high density specimen, air anneal.

species along grain boundaries. The absence of any carbonaceous vapor species such as C or CO in the alumina die modified the reactions.

Samples from the disk formed in the alumina die remained white after upon annealing in air and vacuum. The high density second sample showed a clouding of the center region presumably due to the formation of pores from entrapped gases, similar to that observed by Rice.[5] The air anneal removed the grayish core from the sample hot pressed in the graphite die, and the resulting piece was uniformly white with little evidence of clouding. This difference in clouding of the air annealed specimen was most likely attributable to the ability of the porous graphite die to remove more of the gaseous species formed during the pressing. The chemical nature of the residue along grain boundaries in the two specimens could also have been different because of the difference in ambient atmospheres during hot pressing; this difference then, would be responsible for the nature of gas producing reactions on annealing in air.

The vacuum annealed specimen from the graphite die retained a faint gray core of about the same proportions; however, the core lost its slight translucency. The sample annealed in the die was gray throughout, and exhibited a much higher weight loss than the samples annealed in air or vacuum in the absence of graphite. Since the weight loss was much greater than that in vacuum, it could not be attributed solely to the volatilization of MgO, and was most likely due to reduction of MgO by carbon or CO.

The optical micrographs in Fig. 11 show the similarity in the microstructures of the annealed specimens from the graphite die. The average grain size was essentially constant in each case, but the number and

size of pores varied. The pores were predominantly on grain boundaries; in the die annealed specimen, however, the pores were somewhat larger and located primarily at triple points.

As shown in the micrographs of Fig. 12, the annealed specimens from the alumina die were also similar but showed a considerable increase in grain size over those produced from the graphite die. This emphasized the fact that the nature of the grain boundary impurity and structure after hot pressing in the graphite die had a greater effect on the retardation of grain growth during annealing. It is also interesting to note that the grain size for the annealed specimens from the alumina die was larger than that for the annealed specimens from unmilled powder hot pressed in the graphite die.

(b) Type II MgO

Table IV also contains data on weight loss on annealing, density and grain size for Type II MgO specimens fabricated in both dies, and annealed in various ambient atmospheres. As before, these specimens were fabricated using procedure (2). The as-hot-pressed fracture surfaces are shown in Fig. 13, and the polished sections of the annealed specimens are shown in Figs. 14 and 15.

The specimen hot pressed in the graphite die was gray across its entire cross section, and was translucent; in the alumina die, the specimen was white and translucent. Samples from both dies were white after annealing in air and showed considerable clouding in their centers. A significant decrease in density occurred on annealing, and white spots up to 3 mm in diameter developed just under the surface. These spots were primarily planar and perpendicular to the hot pressing direction,

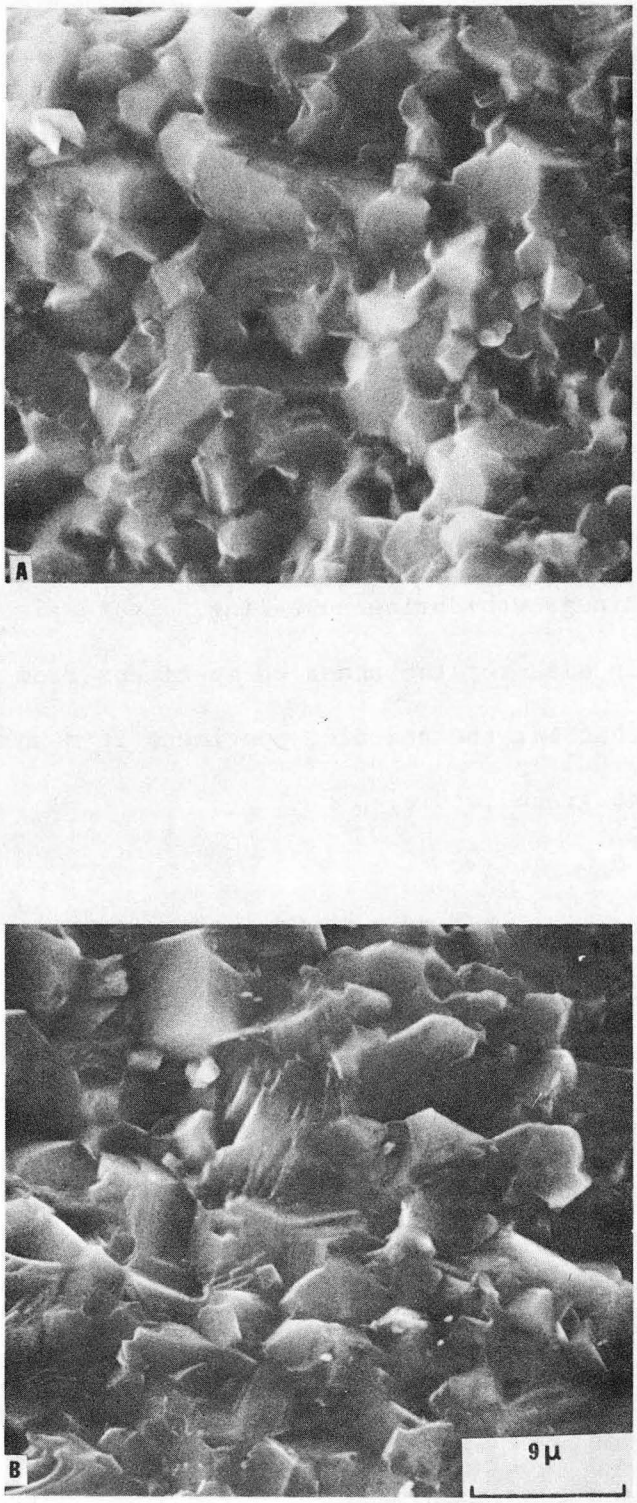

XBB 748-5189

Fig. 13. As-hot-pressed fracture surfaces of Type II MgO specimens: (a) graphite die, (b) alumina die.

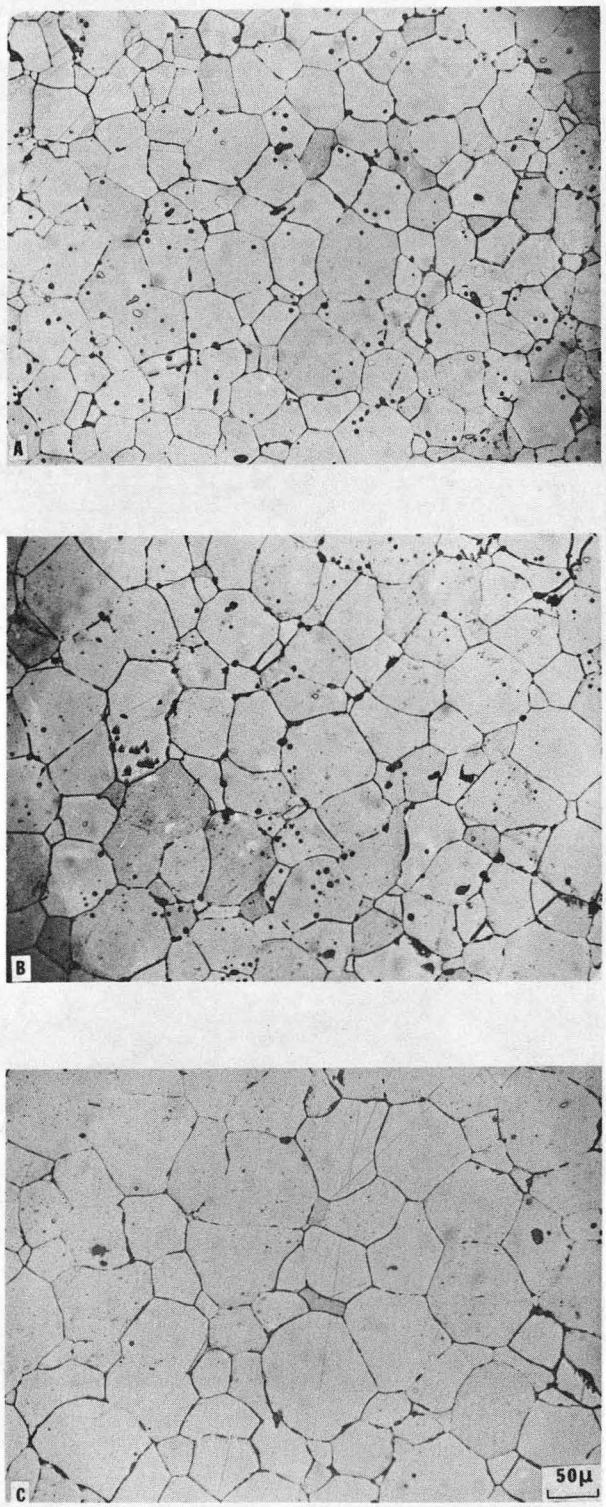

XBB 748-5187

Fig. 14. Micrographs of annealed Type II specimens from graphite die: (a) air anneal, (b) vacuum anneal, (c) die anneal.

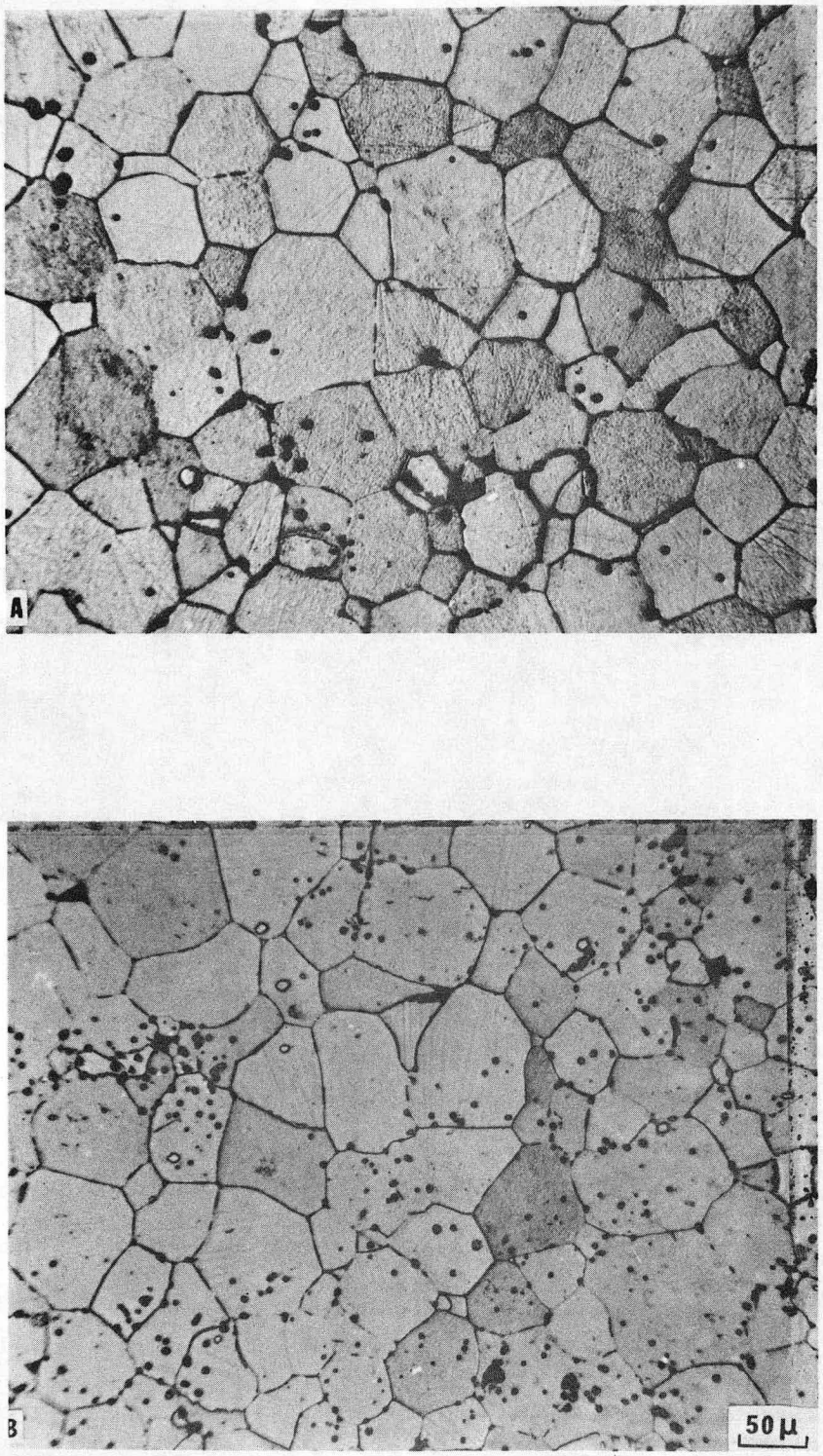

XBB 748-5191

Fig. 15. Micrographs of annealed Type II specimens from alumina die: (a) air anneal, (b) vacuum anneal.

but were also seen just under other surfaces. Microscopic examination of the cross-section of the spots showed them to be actual voids between a denser outer layer and the cloudy porous center. It is expected that the higher density of the outer region prevented the escape of gases generated in the interior, resulting in sufficient build-up of pressure to open the voids. Similar spots were seen in the vacuum annealed specimens from both dies, but the spots were smaller and fewer in number. The die annealed specimen (graphite die) was gray throughout and free of spots. The weight loss pattern on annealing was similar to that for Type I MgO specimens.

The TGA results from the powders contributed to an explanation of the more severe clouding observed in Type II MgO samples. As pointed out earlier, Type II MgO powder was still losing weight at 1000°C whereas Type I had nearly stabilized. This weight loss was probably the combined effect of continued removal of hydroxyl groups and the beginning of the sulfate decomposition which has a decomposition temperature of 1124°C. The rapid densification of Type II could lead to the entrapment of undecomposed sulfate, which subsequently decomposed on annealing causing clouding. There are, however, other undetermined reactions in the different ambient atmospheres as indicated by the varying degree of cloudiness and spot formation.

The microstructures for the annealed specimens, Figs. 14 and 15, show that porosity was mainly within the grains for all cases, and there is evidence of a film along grain boundaries. Figure 16 shows a high magnification of the air annealed sample showing conclusively the presence of a second phase. This second phase was attributed to the high Ca and

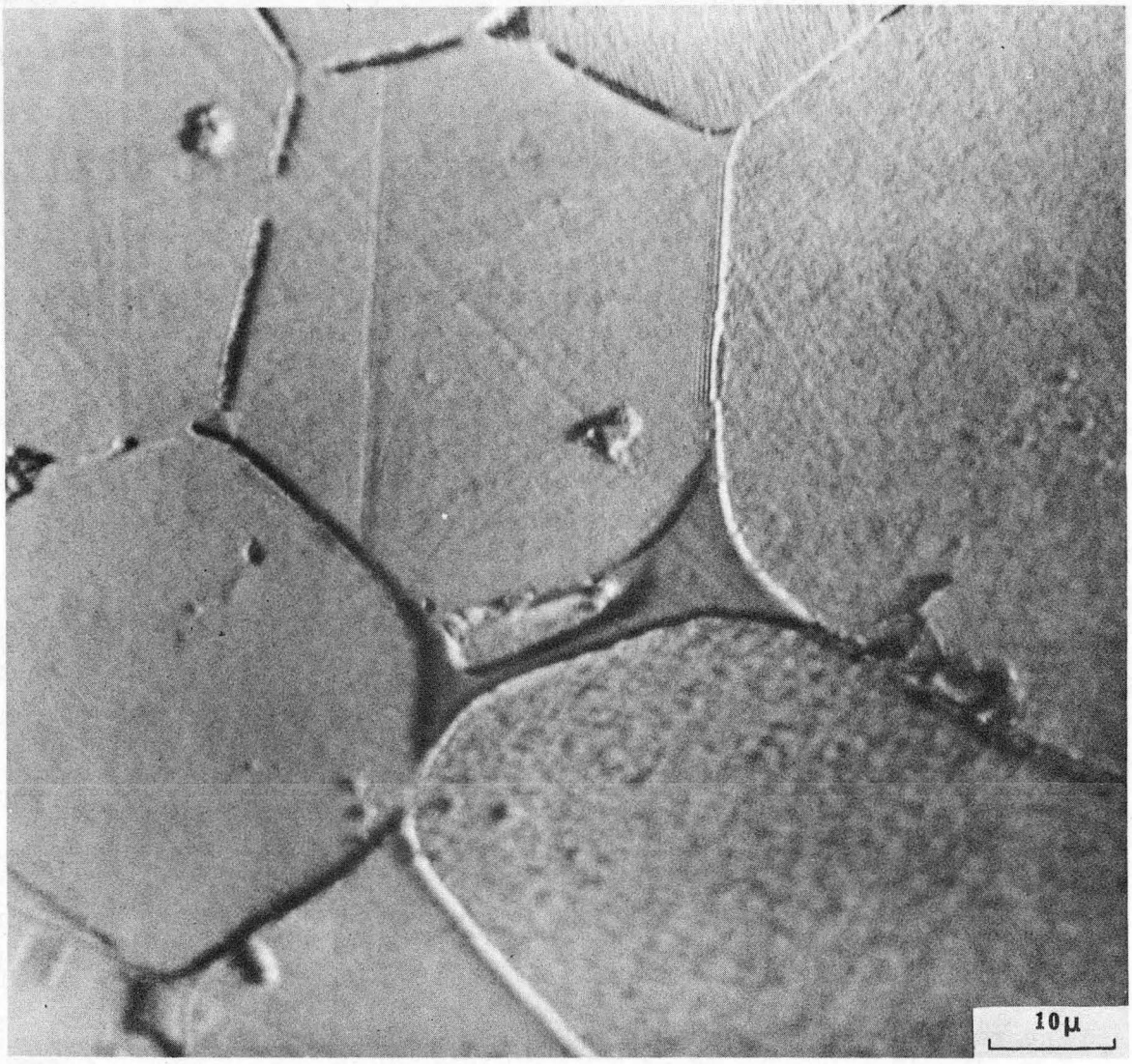

XBB 748-5194

Fig. 16. Micrograph of Type II MgO, graphite die, air anneal.

Si content of the Type II powder leading to the formation of a calcium-magnesium-silicate liquid phase during the high temperature anneal. This liquid phase presumably was responsible for the large increase in grain growth during annealing in comparison with the Type I MgO specimens. A similar effect was observed by Snowden in that with an addition of 5% CMS to MgO, a two-fold increase in grain size was observed over MgO without CMS; subsequent additions to 15%, however, decreased the grain size from the 5% value. Grain growth in the presence of a liquid phase occurs by a solution-precipitation mechanism. For small amounts of liquid phase, where diffusion paths across the liquid phase are small, this process is normally faster than grain growth in the absence of a liquid phase, leading to enhanced grain growth. When the amount of liquid is increased, and thereby the diffusion path, the process is slower with a smaller grain growth rate.

The liquid phase also has apparently eliminated most of the atmospheric effects during hot pressing as subsequently observed in grain growth during annealing since the grain size was similar for all annealed specimens of Type II MgO. For Type I MgO specimens the grain size was larger for the specimens formed by hot pressing in the alumina die.

B. Mechanical Behavior

Stress-strain curves for the annealed specimens from the graphite die of both types of MgO are shown in Fig. 17 and the curves for the air annealed specimens from the alumina die are presented in Fig. 18. The yield stress, maximum stress and plastic strain at maximum stress are summarized in Table V. Fracture surfaces formed by breaking specimens after deformation for both Types I and II, air and die annealed are shown

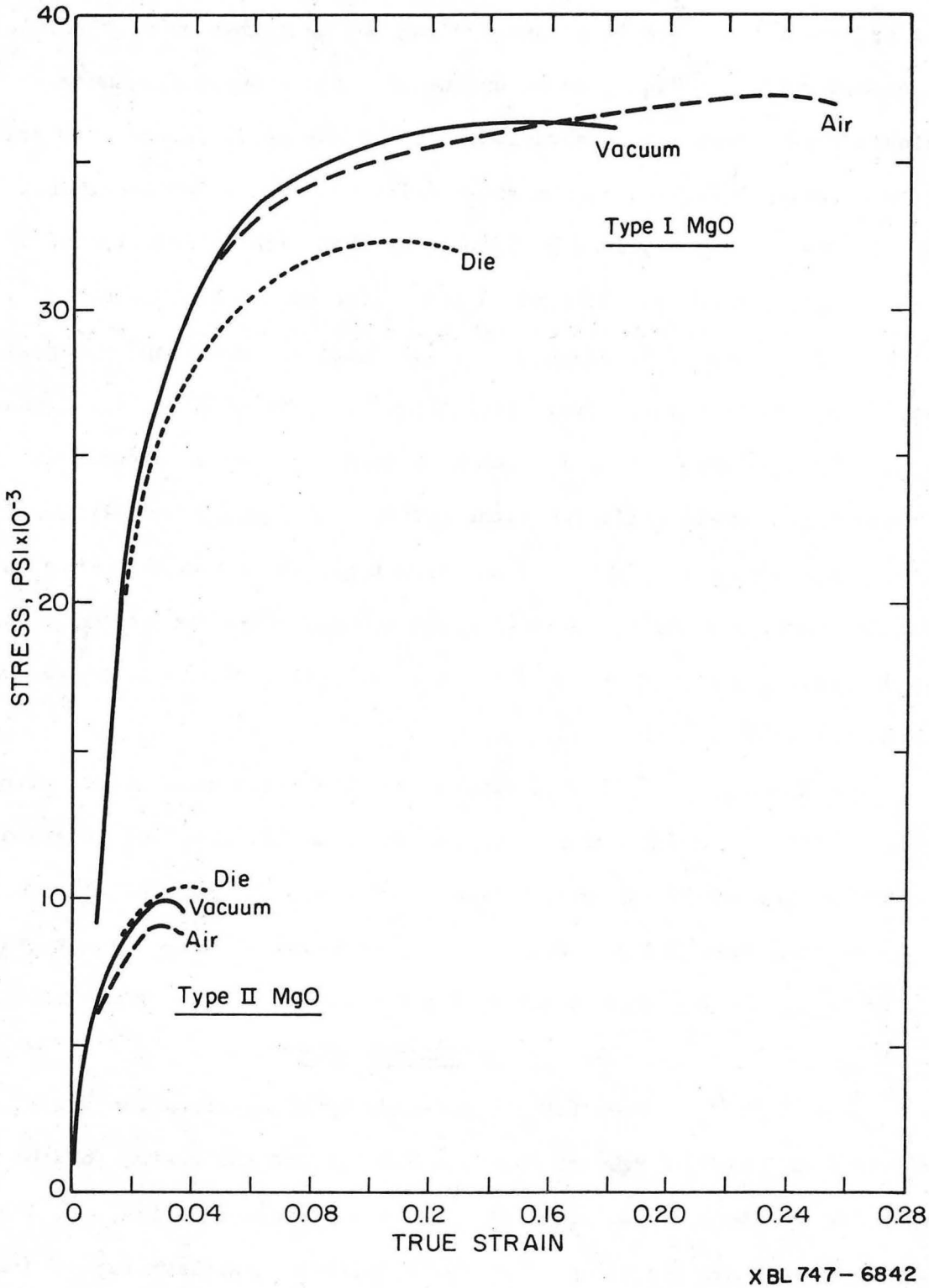

Fig. 17. Stress-strain curves at 1200°C for Types I and II specimens annealed in air, vacuum, and vacuum within the graphite die after hot pressing in graphite die.

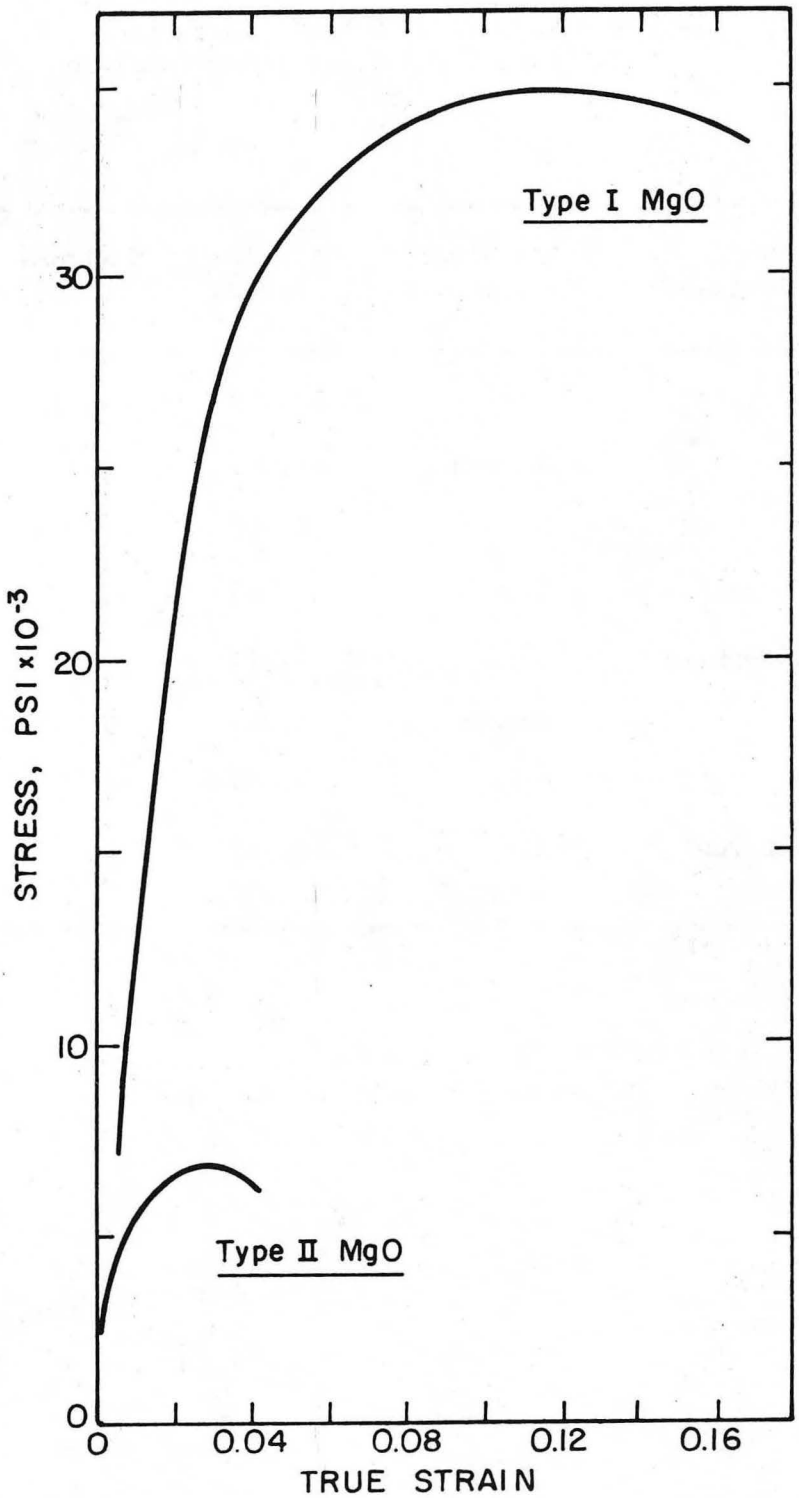

XBL 747-6846

Fig. 18. Stress-strain curves at 1200°C for the high density Type I specimen and the Type II specimen, both annealed in air after hot pressing in alumina die.

Table V. Mechanical behavior data for Type I and Type II MgO specimens

Powder	Die Used	Annealing Environment	Yield Stress	Maximum Stress	Plastic Strain
Type I	Graphite	Air	24,000	37,200	23.4
		Vacuum	24,600	36,400	14.0
		Die	22,800	32,300	8.6
	Alumina	Air	20,000	34,900	10.6
Type II	Graphite	Air	5,300	9,050	2.4
		Vacuum	6,000	9,900	2.4
		Die	6,000	10,050	2.9
	Alumina	Air	4,540	6,850	2.1

Figs. 19-22.

In testing these samples with a constant strain rate, the load increased to the reported maximum, then decreased slowly and finally at an accelerating rate, at which time the test was ended. In this type of test, the recorded load is a measure of the resistance to deformation; the observed decrease in load after the maximum was attributed to the weakening of the specimen due to an increasing population of cracks.

Macroscopic examination of the specimens after testing revealed that all Type I specimens contained visible vertical cracks near the center on one or more faces, whereas Type II specimens had cracks at the corners extending along the vertical length of the sample as shown schematically in Fig. 23. In compression testing, frictional forces develop between the specimen and the ram faces; these constraining forces lead to a barreling type of deformation which develops tensile stresses perpendicular to the loading direction, and regions of high strain on the faces. Type II samples which showed little ductility, could not accommodate this high strain at the edges, and produced fractures as illustrated. In contrast, Type I samples which exhibited much more ductility could accommodate the strain at the edges by yielding in shear, and eventually began to fail by producing fractures in the center, which was the region of maximum tensile stress.

True plastic deformation of polycrystalline MgO requires the movement of five independent slip systems according to the Von Mises criteria for plasticity.[56] At 1200°C, dislocations can move first in favorably oriented grains on three (110) $\langle 1\bar{1}0 \rangle$ slip systems for which the yield stress for a conjugate pair is about 3000 psi at a stress rate of 20

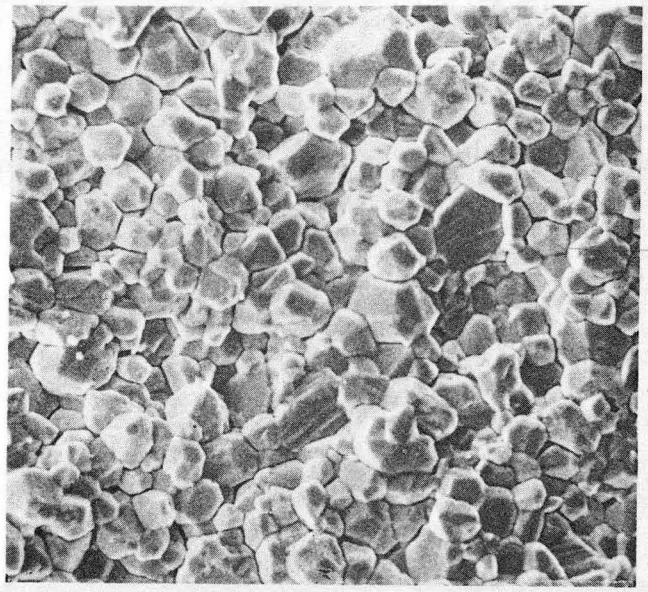

Fig. 19. Fracture surface after deformation of Type I MgO hot pressed in graphite die and annealed in air.

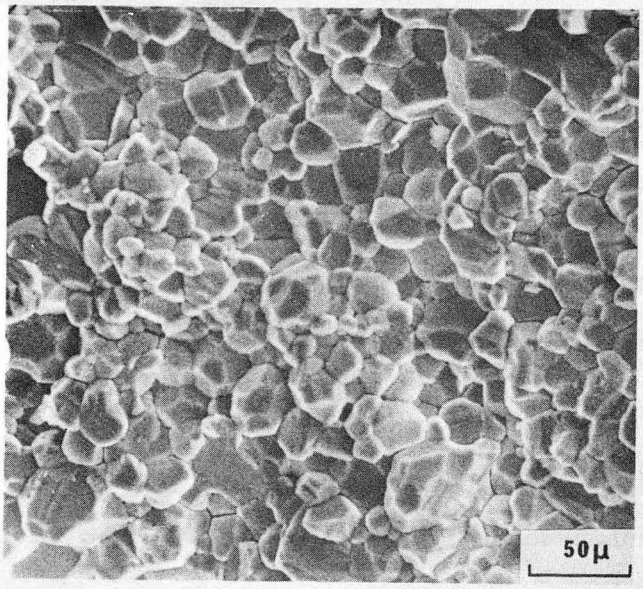

XBB 748-5192

Fig. 20. Fracture surface after deformation of Type I MgO hot pressed in graphite die and annealed in vacuum within the graphite die.

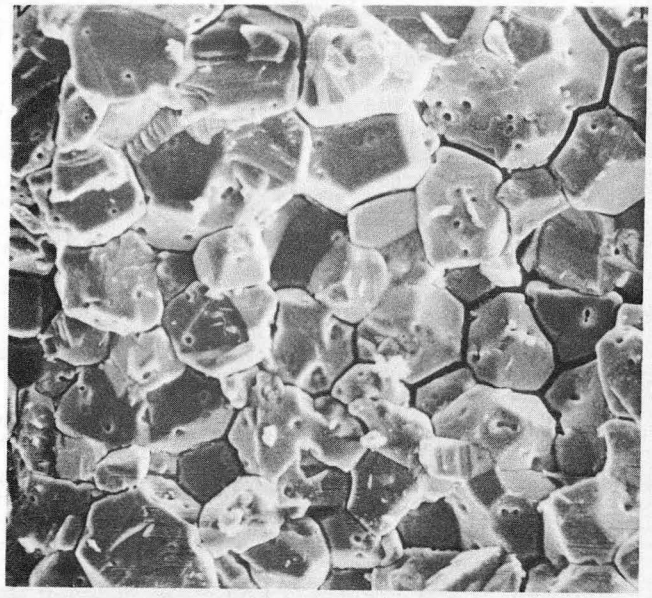

Fig. 21. Fracture surface after deformation of Type II MgO hot pressed in graphite die and annealed in air.

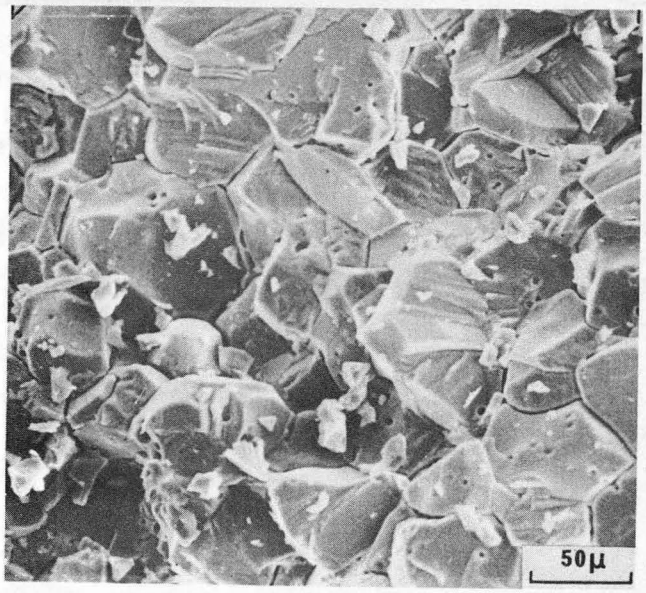

XBB 748-5190

Fig. 22. Fracture surface after deformation of Type II MgO hot pressed in graphite die and annealed in vacuum within the graphite die.

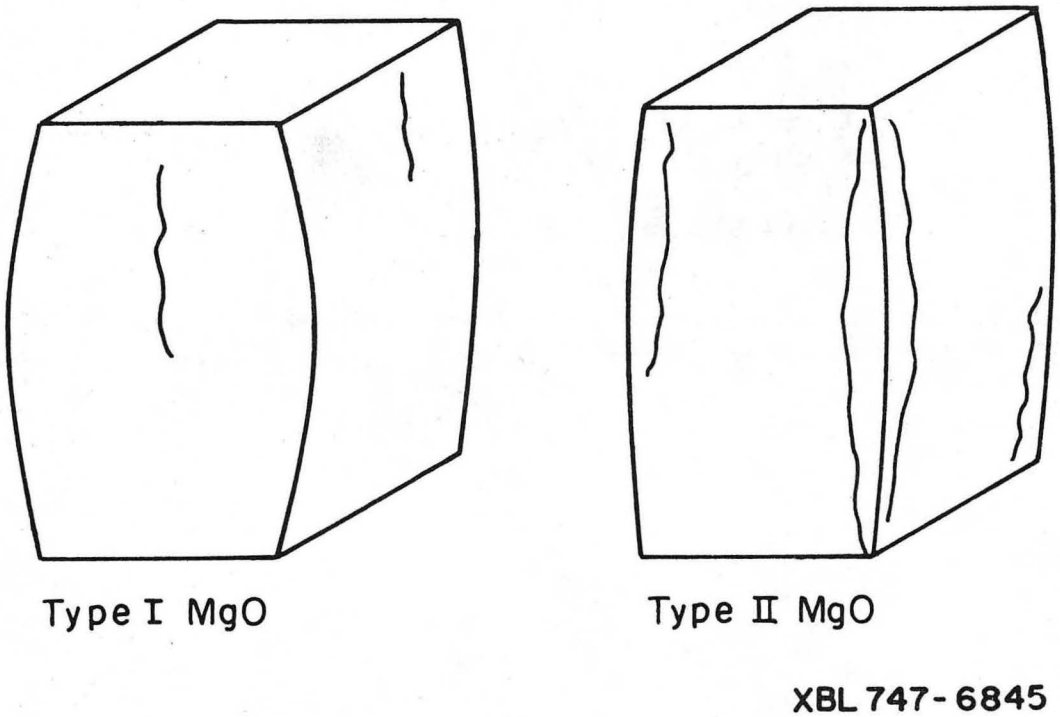

Fig. 23. Schematic diagram of cracking seen after stress-strain testing in Types I and II MgO.

psi/sec.;[30] adjacent grains, however, may not be suitably oriented to allow the dislocations to move through the boundary, resulting in dislocation pile-ups, which leads to stress concentrations. If the specimen has boundaries low in impurity and porosity which are thereby strong enough to maintain integrity to higher stress levels, stress levels may be reached to initiate slip on two secondary (100) $\langle 1\bar{1}0 \rangle$ systems, for which the yield stress is about 18,000 psi at 1200°C at a stress rate of 20 psi/sec,[30] in favorably oriented grains resulting in plastic deformation. If the stress concentrations cannot be relieved completely by flow in adjacent grains, cracks may be nucleated at the grain boundary; or if the grain boundaries should be weak, cracks may form at grain boundaries before plastic flow is realized in adjacent grains. These cracks, however, may not lead to direct propagation and failure depending on the nature of the specimen.

Examining the mechanical behavior of the Type I specimens from the graphite die (Fig. 17), the data show the yield stresses were similar yet the plastic strain was quite different, the air annealed specimen showing nearly three times the strain as the die annealed. Since the microstructure, including grain size and the amount and distribution of pores was similar in each case, the significant variable must have been the nature of the grain boundary after annealing. The air annealed specimen which was exposed to a high partial pressure of oxygen during the heat treatment presumably had a grain boundary character relatively free of impurities because of the oxidizing atmosphere. In the die annealing, the ambient atmosphere was free of oxygen and probably consisted mainly of CO, and therefore the specimen would be expected to contain much of

the impurities initiated by processing and hot pressing in a graphite die. The vacuum annealed specimen would be expected to have grain boundaries of purity intermediate to the air and die annealed. This variation of grain boundary structure correlates with the amount of plastic strain at the maximum stress. The high yield stresses for these specimens in comparison with those for the slip systems suggests the presence of grain boundaries in all cases that offer some resistance to nucleation and transmission of slip; there is also the possibility that the higher strain rates in this study could have contributed to the higher yield stresses.

In the air annealed graphite die Type I MgO specimen which presumably had the strongest grain boundaries, initial dislocation movement resulted in some plastic deformation; cracks, however, began to develop between the most unfavorably oriented grains. These cracks did not readily propagate because of strong grain boundaries. Continued stress concentrations resulted in accommodation by some localized plastic deformation and progressive grain boundary separation akin to crack branching. The die annealed specimen, on the other hand, could not accommodate the initial cracks as easily because of weaker grain boundaries; therefore, it is expected that once the cracks were initiated their propagation was more probable, leading to their easier growth and linkage with other cracks, and eventually forming a crack of critical length. The SEM photographs in Figs. 19 and 20 support this analysis. As seen in Fig. 19, the fractured surface of the air annealed specimen showed considerable cracking and boundary separation; the die annealed specimen, Fig. 20, showed little spearation and fewer cracks.

The Type I air annealed sample from the alumina die appears to deviate from this argument in that it was expected to contain the least amount of impurities and therefore the strongest grain boundaries, but it was closest in mechanical behavior to the graphite die specimen annealed in the graphite die (Figs. 17 and 18). The grain size, however, is 33% larger in this specimen. Vasilos et al.[43] reported a decrease in strength with increase of grain size, and Evans et al.[47] showed a decrease in stress to initiate cracks by grain boundary pile-up with increasing grain size. Thus, increasing grain size increases the probability of forming a crack that will propagate to failure more readily because of its larger size. The effect of grain size is discussed further in the following paragraph.

The behavior of the Type II MgO specimens was markedly different from that of Type I but similar to each other (Figs. 17 and 18). This relationship was attributed to two factors: the large grain size, and the presence of the second phase. The existence of the second phase was further verified by the debris on the fracture surfaces, as seen in Figs. 21 and 22. The second phase itself does not explain the decrease in yield stress since Snowden[49] reported a slight increase in the compressive yield stress of specimens with a 5% addition of CMS at 1200° (specimens had an average MgO grain size of 30 μm), and attributed it to the interference of dislocation motion across grain boundaries.

In this case, the large grain size apparently was the dominating factor in the behavior of Type II MgO and the effects of possible grain boundary structure differences were not dominant. The effect of grain size on yield stress in metals has been described by Petch,[57] and an

inverse square root relationship was found. A similar effect has been noted in MgO as previously mentioned. For a given stress, the large grained Type II could have more dislocation pile-ups per grain than the smaller Type I. Also, the piling-up was enhanced by the presence of the brittle second phase which inhibited dislocation nucleation and motion across the boundary. The resulting high stress concentrations were accommodated by the formation of cracks, which can be large in a large grain material. These long cracks led to failure at much lower stress levels and low strains.

V. SUMMARY AND CONCLUSIONS

Specimens were fabricated from two different MgO powders prepared by dispersing in isopropanol, drying, and milling in a rubber-lined mill with alumina balls, by hot pressing in graphite and alumina dies, followed by annealing in air, vacuum, and within the graphite die in vacuum. Specimens produced from Type I MgO powder had microstructures of varying grain size and grain boundary structure; Type II MgO powder had a small amount of second phase along grain boundaries and considerably larger grains. The specimens were tested in compression at a constant strain rate at 1200°C.

In the Type I specimens the amount of plastic strain was determined by the nature of the grain boundary: the more perfect the boundary, the more strain at failure. This behavior was attributed to the ability of the specimen to accommodate cracks developing during the testing. In specimens with stronger and purer boundaries cracks could be accommodated by localized plastic deformation at the crack tip and by progressive grain boundary separation akin to crack branching. The specimens with more imperfect grain boundaries could not accommodate cracks as easily leading to failure at lower maximum stresses and less strain at maximum stress.

In specimens of Type II MgO grain boundary modifications during specimen preparation were minimized by the presence of a second phase and the detrimental effects of a large grain size. These specimens failed at considerably lower stresses and strains.

The role of impurities in determining the character of the specimens was seen to be significant throughout the entire processing procedure.

The impurities associated with the starting powder were found to be significant in two ways. The presence of anions OH^-, $SO_4^=$ and $CO_3^=$ played a role in the production of gases during hot pressing and annealing. The relatively high cation content, particularly Ca and Si, led to the formation of a liquid phase during the annealing step which was distributed along grain boundaries. The impurities introduced during the preparation of the powder were also significant. Rubber contamination, and also teflon if used, during milling in rubber-lined ball mills retarded grain growth, more so with teflon, on subsequent annealing. Grain boundary character was also affected by whether hot pressing was done in a graphite or alumina die. The formation of a liquid phase due to presence of impurities in the powder tended to eliminate the effect of these processing variables. The mechanical behavior, since it is dependent on the character of the specimen, was correspondingly affected.

It is seen that in developing microstructures of controlled character, the role of impurities introduced either in the powder or in processing is critical. Since the use of ultra high purity powders is impractical in many cases, the understanding and control of processing procedures are essential. Further work is needed to determine the actual reactions taking place during the fabrication processes so that such an understanding can be obtained.

ACKNOWLEDGMENTS

The author would like to sincerely thank Prof. Joseph Pask for his guidance and efforts throughout this investigation.

Discussions with Bill Snowden, Chung Dokko, and Carl Hoge were very helpful and are acknowledged. The suggestions and comments by Prof. Richard Fulrath were also useful and appreciated. The author would also like to thank his friend Dipak Biswas for his advice and support.

The help received from the staff of the Inorganic Materials Research Division of the Lawrence Berkeley Laboratory was appreciated, in particular, the assistance of Kelly Radmilovic, George Georgakopoulos, Lee Johnson, Jack Wodei and Walt Toutolmin. Thanks are also extended to Leonard Lee of Merck and Co. for analytical work on the MgO powders. The author also wishes to express his gratitude to Kaiser Refractories for the financial support of part of this work.

The author would like to acknowledge the assistance and understanding of his wife, Susan D. Sweeting, during the course of this investigation.

This work was done under the auspices of the United States Atomic Energy Commission.

REFERENCES

1. P. Murray, D. Lively, and J. Williams, in Ceramic Fabrication Processes edited by W. Kingery, Technology Press of MIT, Cambridge, and John Wiley and Sons Inc., New York, 1958.
2. T. Vasilos and R. Spriggs, J. Am. Ceram. Soc., 46 [10] (1963).
3. R. Spriggs, L. Brisette, M. Rossetti and T. Spriggs, Am. Ceram. Soc. Bull., 45 [3] (1963).
4. M. Leipold and T. Nielsen, Am. Ceram. Soc. Bull., 45 [3] (1966).
5. R. Rice, "Production of Transparent MgO at Moderate Temperatures and Pressure," presented at 64th Annual Meeting of the Am. Ceram. Soc., New York, N.Y., April 30, 1962, Whitewares Div. No. 5-N-62.
6. S. Copley and J. Pask, J. Am. Ceram. Soc., 48 [12] (1965).
7. G. Miles, R. Sambell, J. Rutherford and G. Stephenson, Trans. Brit. Ceram. Soc., 66 p. 319 (1967).
8. P. Hart, R. Atkin and J. Pask, J. Am. Ceram. Soc. 53 [2] (1970).
9. R. Shelley and P. Nicholson, J. Am. Ceram. Soc. 54 [8] (1971).
10. M. Leipold and C. Kapadia, J. Am. Ceram. Soc., 54 [8] (1971).
11. R. Rice, Proc. Brit. Ceram. Soc., 12, p. 99 (1969).
12. T. Nielsen and M. Leipold, J. Am. Ceram. Soc. 46 [8] (1963).
13. R. Day and R. Stokes in Materials Science Research, Vol. 3 edited by W. Kriegel and H. Palmour III, Plenum Press, New York, 1966.
14. M. Leipold, J. Am. Ceram. Soc., 49 [9] (1966).
15. A. Gorum, E. Parker and J. Pask, J. Am. Ceram. Soc., 41 [5] (1958).
16. E. Parker, J. Pask, J. Washburn, A. Gorum and W. Luhman, J. Metals, 10, p. 351 (1958).

17. A. E. Gorum, W. J. Luhman and J. A. Pask, J. Am. Ceram. Soc., 43 [5] (1960).

18. R. Stokes, T. Johnson and C. Li, Phil. Mag., 4, p. 920 (1959).

19. J. Washburn, A. Gorum, E. Parker, Trans. AIME, 215 [2] (1959).

20. W. Johnson, Phil. Mag., 5, p. 735 (1960).

21. R. Stokes, T. Johnson and C. Li, Phil. Mag., 4, p. 137 (1959).

22. R. Stokes, T. Johnson and C. Li, Phil. Mag., 3, p. 718 (1958).

23. J. Washburn and A. Gorum, Mem. Sci. Rev. Met., 57, p. 67 (1960).

24. R. Stokes, T. Johnson and C. Li, Trans. AIME, 215, p. 437 (1959).

25. F. Clark and R. Sambell, Phil. Mag., 5, p. 697 (1960).

26. R. Stokes, T. Johnson and C. Li, Phil. Mag., 6, p. 9 (1961).

27. R. Stokes and C. Li, J. Am. Ceram. Soc., 46 [9] (1963).

28. J. May and L. Kronberg, J. Am. Ceram. Soc., 43 [10] (1960).

29. C. Hulse and J. Pask, J. Am. Ceram. Soc., 43 [7] (1960).

30. C. Hulse, S. Copley and J. Pask, J. Am. Ceram. Soc., 46 [7] (1963).

31. S. Copley and J. Pask, J. Am. Ceram. Soc., 46 [7] (1963).

32. R. Day and R. Stokes, J. Am. Ceram. Soc., 47 [10] (1964).

33. R. Day and R. Stokes, J. Am. Ceram. Soc., 49 [2] (1966).

34. G. Miles, F. Clark, B. Henderson and R. King, Proc. Brit. Ceram. Soc. 6, p. 325 (1966).

35. R. Moon and P. Pratt, Proc. Brit. Ceram. Soc., 15, p. 203 (1970).

36. M. Srinivasan and T. Stobe, J. Mat. Sci., 9, p. 121 (1974).

37. A. Westwood, Phil. Mag., 6, p. 195 (1962).

38. T. Johnston, R. Stokes and C. Li, Phil. Mag., 7, p. 23 (1962).

39. H. Sinha, Phil. Mag., 8, p. 2115 (1963).

40. M. Adams and G. Murray, J. Appl. Phys., 33, p. 2126 (1962).

41. G. Murray, J. Am. Ceram. Soc., 43 [6] (1960).

42. A. Mountvala and G. Murray, Phil. Mag., 13, p. 441 (1966).

43. T. Vasilos, J. Mitchell and R. Spriggs, J. Am. Ceram. Soc., 47 [12] (1964).

44. R. Day and R. Stokes, J. Am. Ceram. Soc., 49 [7] (1966).

45. T. Langdon and J. Pask, J. Am. Ceram. Soc., 54 [5] (1971).

46. A. Evans and R. Davidge, Phil. Mag., 20, p. 373 (1969).

47. A. Evans, D. Gilling and R. Davidge, J. Mat. Sci., 5, p. 187 (1970).

48. W. Snowden and J. Pask, Phil. Mag., 29, p. 441 (1974).

49. W. Snowden, M.S. Thesis, Univ. of Calif., UCRL-20567, June 1971.

50. G. Terwilliger and K. Radford, Am. Ceram. Soc. Bull., 53 [2] (1974).

51. K. Radford and G. Terwilliger, Am. Ceram. Soc. Bull., 53 [6] (1974).

52. R. Bennett and D. Niesz, Office of Naval Research, Contract No. N00014-68-C-0342, NRO 32-511, July 1973.

53. J. Chown and R. Deacon, Trans. Brit. Ceram. Soc., 63 [2] (1964).

54. R. Rau, J. Cryst. Rev., 3, p. 212 (1961).

55. Merck Index, 8th Edition, Edited by P. Stecher, Merck & Co., Rahway, N.J., Copyright 1968.

56. R. von Mises, Z. Angew. Math. Mech., 8, p. 161 (1928).

57. N. Petch, Prog. Met. Phys., 5 (1956).

LEGAL NOTICE

This report was prepared as an account of work sponsored by the United States Government. Neither the United States nor the United States Atomic Energy Commission, nor any of their employees, nor any of their contractors, subcontractors, or their employees, makes any warranty, express or implied, or assumes any legal liability or responsibility for the accuracy, completeness or usefulness of any information, apparatus, product or process disclosed, or represents that its use would not infringe privately owned rights.

TECHNICAL INFORMATION DIVISION
LAWRENCE BERKELEY LABORATORY
UNIVERSITY OF CALIFORNIA
BERKELEY, CALIFORNIA 94720